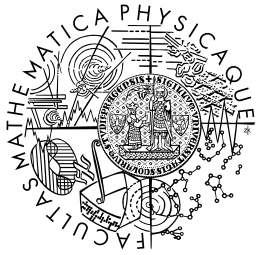

FACULTY
OF MATHEMATICS
AND PHYSICS
Charles University

BACHELOR THESIS

Tomáš Trachta

Structure of a boundary layer between a star and an accretion disk: analytical models

Institute of Theoretical Physics

Supervisor of the bachelor thesis: RNDr. Jiří Horák, Ph.D.

Study programme: Physics

Study branch: FP

Prague 2023

I declare that I carried out this bachelor thesis independently, and only with the cited sources, literature and other professional sources. It has not been used to obtain another or the same degree.

I understand that my work relates to the rights and obligations under the Act No. 121/2000 Sb., the Copyright Act, as amended, in particular the fact that the Charles University has the right to conclude a license agreement on the use of this work as a school work pursuant to Section 60 subsection 1 of the Copyright Act.

In ..... date ....

Author's signature

I want to express sincere gratitude towards my supervisor RNDr. Jiří Horák, Ph.D. for his patience, leadership and invaluable help he has provided me with throughout this work. I am also thankful to my family and friends, whose emotional support helped me finish this thesis.

Název práce: Struktura okrajové vrstvy mezi hvězdou a akrečním diskem: analytické modely

Autor: Tomáš Trachta

Ústav: Ústav teoretické fyziky

Vedoucí bakalářské práce: RNDr. Jiří Horák, Ph.D., Astronomický ústav Akademie věd České republiky

Abstrakt: V této práci se pokoušíme najít trojrozměrné řešení Navier–Stokesových rovnic popisujících α–disk akreující na neutronovou hvězdu. Řešení pro velké radiální vzdálenosti je dobře známé, nicméně vede k singularitě na poloměru, kde je silový moment nula. Na okolí tohoto poloměru se vytvoří okrajová vrstva, jelikož řešení pro velké radiální vzdálenosti nemůže splnit vnitřní okrajové podmínky, tudíž toto řešení přestává být platné. Matematicky jde o singulární perturbace. Abychom se zbavili této singularity, použijeme metodu napojených asymptotických rozvojů, což vede na nové pohybové rovnice. V první části práce shrnujeme známé výsledky, které nám pomohou s argumenty pro přeškálování rovnic. Ve druhé části škálujeme rovnice a pokoušíme se je vyřešit.

Klíčová slova: hydrodynamika, akrece, poruchové metody

Title: Structure of a boundary layer between a star and an accretion disk: analytical models

Author: Tomáš Trachta

Institute: Institute of Theoretical Physics

Supervisor: RNDr. Jiří Horák, Ph.D., Astronomical Institute of the Czech Academy of Sciences

Abstract: In this work, we attempt to find a three-dimensional solution to the Navier–Stokes equations describing an α–disk accreting onto a neutron star. The solution for great radial distances is well-known. However, this solution leads to a singularity at the zero-torque radius. A boundary layer arises in the neighbourhood of this radius since the solution for great radial distances cannot fulfil the inner boundary condition, therefore it stops being valid. Mathematically we are dealing with singular perturbations. In order to eliminate this singularity, we will use the method of matched asymptotic expansions, which leads to new equations of motion. First, we review known results, then we provide arguments for rescaling the equations of motion, and we attempt to solve the rescaled equations.

Keywords: hydrodynamics, accretion, perturbation methods

Contents

Introduction

Neutron stars are some of the most extreme objects in the universe. The first experimental evidence of neutron stars can be back traced to the 1960s, although their existence was theoretically predicted 30 years prior by Baade and Zwicky [1934]. Some experimental evidence comes from spectral analysis of X-rays emerging from systems containing these stars. Strong X-ray radiation is frequently observed in low mass X-ray binary systems, in which the donor star transfers its mass to a compact object, such as a black hole or a neutron star, creating an accretion disk (see Figure 1 for artist's impression). In the accretion process, a significant fraction of the total energy of the accreted material is converted to radiation, frequently reaching significant fractions of its rest-mass energy, given by probably the most famous equation in physics, $E = mc^2$. In fact, such high efficiency of conversion is far beyond the current technical abilities of the human race. The efficiency of chemical reactions when burning coal is around 10^{-10}, and in nuclear reactors the efficiency reaches 0.001. Accretion efficiency also significantly exceeds the efficiency of nuclear fusion in future fusion reactors, or in the stars, which is estimated to be around 0.007 (these values were taken from Kato et al. [2008]).

The primary source of the energy release in accretion disks is the potential energy of the matter in a strong gravitational field surrounding a compact object (neutron star). To illustrate our point, let us imagine a compact object of mass M accreting a test particle of mass m with zero total mechanical energy. In accretion disks, the particles descend in the gravitational field towards the centre on nearly circular orbits. At distance r from the central object, we can calculate the particle's potential energy as $V = -GMm/r$ and its kinetic energy on the circular orbit as $T = GMm/(2r)$ (we chose to work with Newtonian gravity for simplicity). The total mechanical energy of the particle therefore is $-GMm/(2r)$. Half of the difference of the potential energy of the particle has been converted to the kinetic energy, and the other half has to be converted to other non-mechanical types of energy. The amount of energy that has to be converted gets higher as the material gets deeper in the gravitational field. For a sufficiently compact object with the inner edge of the disk being close enough, the amounts of energy that have to be converted are huge. This is satisfied for both the black holes as well as the neutron stars, which are extremely dense and can have very small radii on the order of 10 kilometres.

For the case of non-rotating black hole, the accretion disk terminates at the innermost stable circular orbit located at $3R_\mathrm{s}$, where $R_\mathrm{s} = 2GM/c^2$ is the Schwarzschild radius. Inside this orbit, the matter starts to fall freely on the black hole, approximately conserving the mechanical energy and the angular momentum. This leads to an efficiency of around 0.06 (Kato et al. [2008]). If the black hole is spinning, the efficiency of accretion grows as the innermost stable circular orbit gets closer to the black hole and particles in the disk can achieve larger difference in potential energies. The efficiency increases up to 0.42 for a maximally rotating Kerr black hole, for which the innermost stable circular orbit is at $R_\mathrm{s}/2$ (Kato et al. [2008]). The innermost regions of black-hole accretion disk have recenetly been resolved by the Event Horizon Telescope, see Figure 2.

Neutron star accretion disks can be even more efficient than black holes at this energy conversion due to the presence of a boundary layer, where the accreted mass has to radiate most of its energy. The luminosity in the boundary layer is proportional to $(\Omega_{\mathrm{K}*} - \Omega_*)^2$ (Shakura and Sunyaev [1988]), where $\Omega_{\mathrm{K}*}$ is the Keplerian angular velocity at the stellar radius and Ω_* is the stellar angular velocity. If one includes relativistic effects, the luminosity of a boundary layer may exceed the luminosity of the rest of the accretion disk. The cause of this luminosity is following. Far from the star, the matter orbits with nearly Keplerian velocity. However, as the matter aproaches the stellar surface, its rotation has to slow down to the spin frequency of the star. This happens in a rather narrow region in the vicinity of the star, where the matter has to lose a significant amount of its kinetic energy. That is why we are interested in the structure of the boundary layer for a neutron star.

In standard accretion disks, proposed by Shakura and Sunyaev [1973], the excess of the mechanical energy is immediately released in the form of thermal radiation. However, there are other types of so-called radiatively inefficient accretion flows, where the energy is stored in the form of internal energy of the accreted matter. This type of flow is called the advection-dominated accretion flow, ADAF for short. ADAFs were discovered by Narayan and Yi [1994], see Kato et al. [2008] chap. 9 for an overview. Another model is the slim-disk model (Abramowicz et al. [1988]). In this model, the accretion rate exceeds a critical accretion rate making the standard model unusable. Part of the energy is stored in the energy of radiation trapped inside the accretion flow. These disks are highly luminous and stable with respect to the thermal instability. We again refer to Kato et al. [2008] for more information. There are also other types of disk models; however, in this work, we make the same assumptions as Shakura and Sunyaev [1973] that all the mechanical energy the material has to lose is locally converted into thermal radiation that immediately leaves the disk.

In general, the structure of the accretion flow is determined by a few parameters, namely mass M of the central object, accretion rate $\dot{M}$, which measures the amount of matter that falls to the central object per unit time, and the viscosity parameter α, which describes the magnitude of friction between adjacent layers of the disk. This friction realises the process of angular momentum transfer. In the standard model, the faster rotating inner layer is losing angular momentum through viscous interaction with the slower rotating adjacent outer layer causing the mass to fall towards the centre while the momentum is transferred outwards. Molecular viscosity on its own would not be enough to drive accretion in Keplerian disks, hence a turbulence in the disk must occur in order to transfer the angular momentum. In the simplest approach of the mixing length theory (Prandtl [1925]), the turbulent angular momentum transfer can be modelled by viscosity with artificial kinematic viscosity coefficient. Shakura and Sunyaev [1973] suggested the kinematic viscosity to be $\nu = \alpha c_{\mathrm{s}}^2/\Omega_{\mathrm{K}}$, where c_{s}^2 is the speed of sound and Ω_{K} is the local Keplerian angular velocity. The parameter α must be less than 1 in order for the turbulent velocity fluctuations to be subsonic. The turbulence also heats the disk up. In the standard-disk model, the local viscous heating calculated with the Shakura-Sunyaev prescription is exactly balanced by radiative losses. The turbulence is crucial in describing the flow as the matter must lose its angular momentum to be able to stay on nearly circular orbits.

The accretion of rotating matter is essentially a two-dimensional problem with mutually connected radial and vertical structure of the disk. However, in most disk models, the vertical structure of the disk is oversimplified. The authors usually simplify the vertical structure by a priori assuming vertical hydrostatic equilibrium. Vertical structure found this way is then averaged over the thickness of the disk and the vertically integrated quantities are used in the equations for the radial structure. In fact, this treatment replaces the original problem that is two-dimensional by two separated one-dimensional problems without solving the two-dimensional structure properly.

Kluźniak and Kita [2000] found self-consistent equations that take vertical structure fully into account for an α-disk. In their equations, the vertical hydrostatic equilibrium is a natural part of the solution and does not need to be assumed a priori. Their solution works well far from the central object but leads to a singularity at the radius, where the torque of the viscous force vanishes. This singularity is caused by the implicit assumption that the quantities describing the disk structure change in the radial direction on a much larger scale than in the vertical direction. This is no longer true when the radial coordinate approaches the zero torque radius. This radius lies in the vicinity of the marginally stable radius for the case of a black hole, where a transition zone arises. In the case of a neutron star, a boundary layer arises as the zero-torque radius is close to the stellar surface. Boundary layers have already been examined in papers such as Shakura and Sunyaev [1988], Regev [1983] and more, but they were mostly studied with the simplifying assumption of vertical hydrostatic equilibrium. Our primary focus in this work will be a model of the boundary layer with self-consistent treatment of the vertical structure.

This thesis is organised in the following manner. In the first chapter, we discuss the assumptions we make and the governing equations. From these equations stem two constants of integration, which we derive in the first chapter as well. We then non-dimensionalise the equations of motion in order to obtain the well-known outer disk solution. In the second chapter, we find the solution valid sufficiently far from the zero-torque radius ("outer-disk solution"), which is in accordance with Kluźniak and Kita [2000]. We also find a prescription for the disk semi-thickness, which helps us to discuss the origin of the singular behaviour of this solution. In the third chapter, we introduce briefly the concept behind the singular perturbation theory, namely matched asymptotic expansions. Then we attempt to make arguments for appropriate rescaling of the equations in order to find a non-singular solution for the flow in the boundary layer. We later propose an ansatz for the solutions and try to solve these equations. Finally, we arrive at a single nonlinear ODE, which has to be solved numerically.

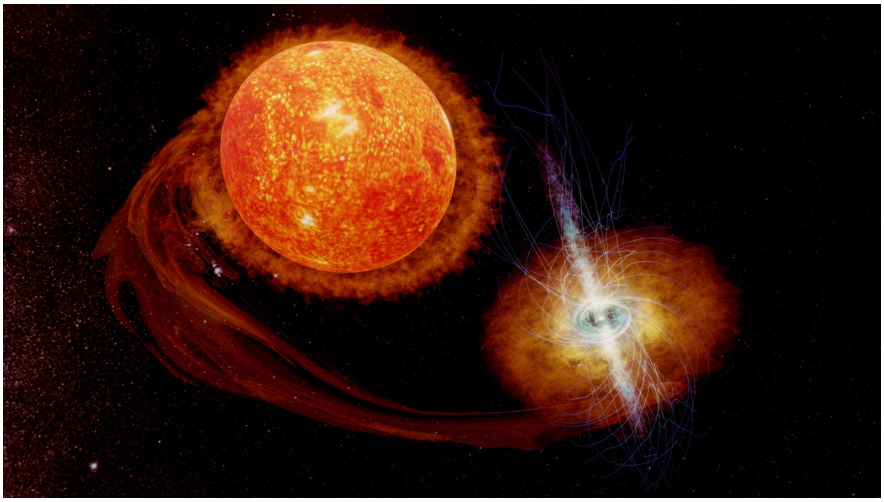

Figure 1: Artist's impression of a Low-Mass X-Ray Binary system, taken from Orlando [2020].

Figure 2: The first ever image of a black hole in Messier 87 captured by the Event Horizon Telescope, which demonstrates the power of accretion disks. (Credit: EHT collaboration)

1. Preliminaries

1.1 Assumptions for disk equations

Our assumptions for the outer solution will not differ much from the assumptions of Kluźniak and Kita [2000] (we will further refer to them as KK). We will use the cylindrical coordinates (r, φ, z) and Newtonian gravity. The assumptions will be as follows:

1. The disk is axisymmetric.

2. Gravitational potential acting upon a fluid element can be described by the Newtonian potential as

$$\psi(r, z) = -\frac{GM}{\sqrt{r^2 + z^2}}, \tag{1.1}$$

   where G is the gravitational constant and M is the mass of the star.

3. The disk is in a steady state.

4. The disk is geometrically thin; we can write this at any given radius r as $H(r) \ll r$, where $H(r)$ is the semi-thickness of the disk at radius r.

5. The radial and the vertical velocities are subsonic inside of the disk.

6. The disk is symmetric under reflection about the mid-plane. Mid-plane is defined by the surface of $z = 0$.

7. We will assume polytropic equation of state for the disk

$$P = K\rho^{(n+1)/n}, \tag{1.2}$$

   where K is a polytropic constant, P is pressure, ρ is the density of the fluid and n is the polytropic index.

8. The turbulent angular-momentum transport can be well described by shear viscosity using the height-dependant version of the Shakura-Sunyaev prescription (Umurhan et al. [2006])

$$\nu = \frac{2}{3}\frac{\alpha}{\Omega_{\mathrm{K}}}\frac{c_{\mathrm{s}}^2}{(1 + 1/n)}, \tag{1.3}$$

   where c_{s} is the local sound speed and the proportionality parameter α is assumed to be constant. The standard version of the viscosity prescription relates the vertically integrated quantities.

A few remarks:

- The assumption 1) means that $\partial/(\partial\varphi) = 0$ and the assumption 3) means $\partial/(\partial t) = 0$.

- The polytropic equation of state means adiabatic flow with entropy constant in both space and time. We will work with $n = 3/2$, which stands for monoatomic gas. The disk has a well-defined boundary given by the semi-thickness H. Outside of the boundary, it holds that $\rho = P = 0$.

- Assumption 2) also assumes that the disk is not self-gravitating. We also ignore any dynamic effects magnetic fields might cause in the disk.

1.2 Governing equations

As the viscosity plays a crucial role in the angular momentum tranport in accretion disks, we will work with Navier-Stokes equations of a viscous fluid and the continuity equation to describe the accretion flow. As we are in fluid dynamics, the complete hydrodynamical system can be described by the density ρ and the velocity field $\overrightarrow{v}$. However, we will use relations ensuing from the polytropic equation of state to describe the system using the local speed of sound c_s instead of the density. The relations are following

$$c_\mathrm{s}^2 = \frac{\mathrm{d}P}{\mathrm{d}\rho} = \left(1 + \frac{1}{n}\right)\frac{P}{\rho}. \tag{1.4}$$

Differentiating equation (1.4) by r and z we get respectively these identities

$$n\frac{\partial c_\mathrm{s}^2}{\partial r} = \frac{1}{\rho}\frac{\partial P}{\partial r}, \tag{1.5}$$

$$n\frac{\partial c_\mathrm{s}^2}{\partial z} = \frac{1}{\rho}\frac{\partial P}{\partial z}. \tag{1.6}$$

We will employ these relations in the future. Next, let us examine the governing equations of motion without these polytropic relations. The equations follow (Kluźniak and Kita [2000])

$$\rho(\overrightarrow{v}\cdot\overrightarrow{\nabla})\overrightarrow{v} = -\overrightarrow{\nabla}P - \rho\overrightarrow{\nabla}\psi + \overrightarrow{\nabla}\cdot\overleftrightarrow{\sigma}, \tag{1.7}$$

$$\overrightarrow{\nabla}\cdot(\rho\overrightarrow{v}) = 0. \tag{1.8}$$

We already disposed of terms involving partial time derivatives. The velocity vector of a fluid element is denoted by $\overrightarrow{v}$, and $\overleftrightarrow{\sigma}$ is the rank-two viscous stress tensor. We can write $\overleftrightarrow{\sigma}$ as (Landau and Lifshitz [1959])

$$\overleftrightarrow{\sigma} = \eta\left(\nabla\overrightarrow{v} + (\nabla\overrightarrow{v})^T\right) + \left(\xi - \frac{2}{3}\eta\right)\overrightarrow{\nabla}\cdot\overrightarrow{v}\,\overleftrightarrow{I}, \tag{1.9}$$

where ξ is the bulk viscosity, η is the dynamic viscosity coefficient, the identity tensor in 3D is denoted by $\overleftrightarrow{I}$ and T denotes transpose of a matrix. For the dynamic viscosity coefficient, we can write $\eta = \nu\rho$, with ν being the kinematic viscosity. We can now express the Navier-Stokes equations in cylindrical coordinates. For a more detailed transformation of these equations see Kato et al.

[2008]. We get the radial, azimuthal and vertical Navier-Stokes equations in cylindrical coordinates, respectively (Kluźniak and Kita [2000])

$$\begin{aligned} v_r\frac{\partial v_r}{\partial r}+v_z\frac{\partial v_r}{\partial z}-\Omega^2 r=-\frac{\partial\psi}{\partial r}-\frac{1}{\rho}\frac{\partial P}{\partial r}+\frac{2}{\rho r}\frac{\partial}{\partial r}\left(\eta r\frac{\partial v_r}{\partial r}\right) \\ -\frac{2\eta v_r}{\rho r^2}+\frac{1}{\rho}\frac{\partial}{\partial z}\left[\eta\left(\frac{\partial v_r}{\partial z}+\frac{\partial v_z}{\partial r}\right)\right]+\frac{1}{\rho}\frac{\partial}{\partial r}\left[\left(\xi-\frac{2}{3}\eta\right)\left(\vec{\nabla}\cdot\vec{v}\right)\right], \end{aligned} \tag{1.10}$$

$$\rho\frac{v_r}{r^2}\frac{\partial}{\partial r}\left(r^2\Omega\right)+\rho v_z\frac{\partial\Omega}{\partial z}=\frac{1}{r^3}\frac{\partial}{\partial r}\left(\eta r^3\frac{\partial\Omega}{\partial r}\right)+\frac{\partial}{\partial z}\left(\eta\frac{\partial\Omega}{\partial z}\right), \tag{1.11}$$

$$\begin{aligned} v_r\frac{\partial v_z}{\partial r}+v_z\frac{\partial v_z}{\partial z}=-\frac{\partial\psi}{\partial z}-\frac{1}{\rho}\frac{\partial P}{\partial z}+\frac{2}{\rho}\frac{\partial}{\partial z}\left(\eta\frac{\partial v_z}{\partial z}\right) \\ +\frac{1}{\rho r}\frac{\partial}{\partial r}\left[\eta r\left(\frac{\partial v_r}{\partial z}+\frac{\partial v_z}{\partial r}\right)\right]+\frac{1}{\rho}\frac{\partial}{\partial z}\left[\left(\xi-\frac{2}{3}\eta\right)\left(\vec{\nabla}\cdot\vec{v}\right)\right], \end{aligned} \tag{1.12}$$

where Ω is the angular frequency, which can be written as $\Omega = v_\varphi/r$. We also chose to write the divergence terms of the viscous tensor in this compact form because, as we will later show, these terms are negligible in the outer disk. We are still missing the continuity equation, so let us examine that. For the continuity equation in cylindrical coordinates, we obtain (Kluźniak and Kita [2000])

$$\frac{1}{r}\frac{\partial}{\partial r}(r\rho v_r)+\frac{\partial}{\partial z}(\rho v_z)=0. \tag{1.13}$$

1.3 Constants of integration

Before we get to solving the equations, we first need to discuss constants of integration as they are crucial in determining the cause of the singularity. Let us vertically integrate continuity equation (1.13). We can write

$$\int_{-\infty}^{\infty}\frac{1}{r}\frac{\partial\left(r\rho v_r\right)}{\partial r}\mathrm{d}z+\int_{-\infty}^{\infty}\frac{\partial\left(\rho v_z\right)}{\partial z}\mathrm{d}z=0. \tag{1.14}$$

The second term is equal to zero as we can write

$$\int_{-\infty}^{\infty}\frac{\partial\left(\rho v_z\right)}{\partial z}\mathrm{d}z=\left[\rho v_z\right]_{z=-\infty}^{z=\infty}=0, \tag{1.15}$$

since $\rho = 0$ for $|z| > H$. We thus get the following

$$\int_{-\infty}^{\infty}\frac{1}{r}\frac{\partial\left(r\rho v_r\right)}{\partial r}\mathrm{d}z=\frac{1}{r}\frac{\partial}{\partial r}\int_{-\infty}^{\infty}r\rho v_r\mathrm{d}z=0. \tag{1.16}$$

Let us now integrate this equation over the azimuthal angle $\varphi \in (0, 2\pi)$. In this step we will also multiply the equation by r giving us

$$2\pi\frac{\partial}{\partial r}\int_{-\infty}^{\infty}r\rho v_r\mathrm{d}z=0. \tag{1.17}$$

We now integrate with respect to r yielding the same result as Kluźniak and Kita [2000]

$$2\pi r \int_{-\infty}^{\infty} \rho v_r \mathrm{d}z = -\dot{M}, \tag{1.18}$$

where $-\dot{M}$ is the integration constant. For accretion, it is conventional in literature such as Frank et al. [2002] to assume $v_r < 0$, meaning $\dot{M} > 0$. Let us now discuss its physical meaning. In the definition of $\dot{M}$, we can see that we are multiplying the integral by the term $2\pi r$, which is the circumference of a circle with radius r. We can also deduce that the integration happens only in the region $(-H, H)$ since the integrand is non-zero in this region and zero everywhere else. The integrand ρv_r gives the radial mass flux. Combined, we get the total amount of mass crossing a cylinder of radius r per unit time. We can see that the mass flowing through a cylinder of any given radius is constant. It is a consequence of the stationarity of the flow since if the amount crossing two cylinders were different, the mass would be steadily accumulated or removed from the volume in between the cylinders.

Let us now discuss another constant of integration. We will obtain this constant by vertically integrating the azimuthal equation (1.11). We can write

$$\begin{aligned}\int_{-\infty}^{\infty} \rho \frac{v_r}{r^2} \frac{\partial}{\partial r}\left(r^2\Omega\right) \mathrm{d}z + \int_{-\infty}^{\infty} \rho v_z \frac{\partial \Omega}{\partial z} \mathrm{d}z = \int_{-\infty}^{\infty} \frac{1}{r^3} \frac{\partial}{\partial r}\left(\eta r^3 \frac{\partial \Omega}{\partial r}\right) \mathrm{d}z \\ + \int_{-\infty}^{\infty} \frac{\partial}{\partial z}\left(\eta \frac{\partial \Omega}{\partial z}\right) \mathrm{d}z,\end{aligned} \tag{1.19}$$

where the last term is zero since we are evaluating $\eta\,(\partial\Omega/\partial z)$ at $\pm\infty$, and, as we have stated before, we can write $\eta = \nu\rho$; therefore, we can use the same argument we did when deriving the first constant of integration. Let us now multiply this equation by r^3 and write it in the following form

$$\int_{-\infty}^{\infty} r\rho v_r \frac{\partial}{\partial r}\left(r^2\Omega\right) \mathrm{d}z + \int_{-\infty}^{\infty} \rho v_z \frac{\partial (r^3\Omega)}{\partial z} \mathrm{d}z = \int_{-\infty}^{\infty} \frac{\partial}{\partial r}\left(\eta r^3 \frac{\partial \Omega}{\partial r}\right) \mathrm{d}z. \tag{1.20}$$

We will now integrate by parts the second term on the left-hand side as follows

$$\int_{-\infty}^{\infty} \rho v_z \frac{\partial (r^3\Omega)}{\partial z} \mathrm{d}z = \left[\rho v_z r^3 \Omega\right]_{-\infty}^{\infty} - \int_{-\infty}^{\infty} r^3 \Omega \frac{\partial (\rho v_z)}{\partial z} \mathrm{d}z. \tag{1.21}$$

The first term on the right-hand side is zero as we are evaluating a term with ρ outside of the disk. We can also rewrite the third term thanks to the continuity equation (1.13) which yields

$$\int_{-\infty}^{\infty} r\rho v_r \frac{\partial}{\partial r}\left(r^2\Omega\right) \mathrm{d}z + \int_{-\infty}^{\infty} r^2\Omega \frac{\partial}{\partial r}\left(r\rho v_r\right) \mathrm{d}z = \int_{-\infty}^{\infty} \frac{\partial}{\partial r}\left(\eta r^3 \frac{\partial \Omega}{\partial r}\right) \mathrm{d}z. \tag{1.22}$$

We can see the product rule being applied on the left-hand side, so we rewrite this equation as

$$\frac{\partial}{\partial r} \int_{-\infty}^{\infty} r^3 \rho v_r \Omega \mathrm{d}z = \frac{\partial}{\partial r} \int_{-\infty}^{\infty} \eta r^3 \frac{\partial \Omega}{\partial r} \mathrm{d}z. \tag{1.23}$$

We now choose to integrate this equation over the azimuthal angle φ and integrate with respect to r yielding

$$2\pi r^3 \int_{-\infty}^{\infty} \rho v_r \Omega \mathrm{d}z + C = 2\pi r^3 \int_{-\infty}^{\infty} \eta \frac{\partial \Omega}{\partial r} \mathrm{d}z, \tag{1.24}$$

where C is an integration constant. We will denote the first term on the left-hand side the same way KK do: $-\dot{J}$. It is important to note that $-\dot{J}$ is a function of r, and its physical meaning is, according to KK, the advection rate of angular momentum through a cylinder of radius r. Let us rewrite the left-hand side as

$$-\dot{J} + C = -\dot{M}(-\langle j \rangle + j_+), \tag{1.25}$$

where we chose $j_+ = C/\dot{M}$ and $\langle j \rangle$ can be written as

$$\langle j \rangle = \frac{2\pi \int_{-\infty}^{\infty} r^3 \rho v_r \Omega \mathrm{d}z}{2\pi \int_{-\infty}^{\infty} r \rho v_r \mathrm{d}z} = \frac{\int_{-\infty}^{\infty} j \rho v_r \mathrm{d}z}{\int_{-\infty}^{\infty} \rho v_r \mathrm{d}z}. \tag{1.26}$$

We can see that $\langle j \rangle$ is equal to the angular momentum $j = r^2\Omega$ unless j is a function of z, or equally, Ω depends on z. In all other cases, $\langle j \rangle$ is the height-averaged specific angular momentum. Let us rewrite the most important result so far

$$\dot{M}(\langle j \rangle - j_+) = -2\pi r^3 \int_{-\infty}^{\infty} \eta \frac{\partial \Omega}{\partial r} \mathrm{d}z. \tag{1.27}$$

1.4 Scaled equations of motion

Our aim is to solve equations (1.10)-(1.13) using the perturbation method. For this we need to write these equations in non-dimensional form and introduce a small dimensionless expansion parameter. In this section, we follow closely KK, and rescale all quantities by their typical values (e.g. values at a typical radius r_* in the disk). We will assume all the dimensionless quantities (except the expansion parameter) to be of the order of unity. We will denote all the typical values with an asterisk as the subscript and all the new non-dimensional variables with a tilde. This will lead to non-dimensional equations in which we can compare the relative significance of every single term. We will use the following scalings:

- radius: $\tilde{r} = r/r_*$,
- vertical coordinate: $\tilde{z} = z/H_*$,
- azimuthal frequency: $\tilde{\Omega} = \Omega/\Omega_* = \Omega/\Omega_{\mathrm{K}}(r_*)$, where $\Omega_{\mathrm{K}}(r_*)$ is the Keplerian azimuthal frequency at the characteristic radius r_*,
- speed of sound: $\tilde{c}_{\mathrm{s}} = c_{\mathrm{s}}/c_{\mathrm{s}*}$,
- radial and vertical velocity: $\tilde{v}_r = v_r/c_{\mathrm{s}*}$; $\tilde{v}_z = v_z/c_{\mathrm{s}*}$, we are scaling all the velocities by the characteristic speed of sound, the same way Regev [1983] does,
- pressure and density: $\tilde{P} = P/(c_{\mathrm{s}*}^2 \rho_*)$; $\tilde{\rho} = \rho/\rho_*$,
- viscosity: $\tilde{\xi} = \tilde{\nu} = \nu/H_* c_{\mathrm{s}*}$; $\tilde{\eta} = \eta/(H_* c_{\mathrm{s}*} \rho_*)$.

Let us remind ourselves what the Keplerian azimuthal frequency at the characteristic radius is: $\Omega_{\mathrm{K}}(r_*) = (GM_*/r_*^3)^{1/2}$. If we assume vertical hydrostatic equilibrium, we can write

$$\Omega_{\mathrm{K}}^2(r_*) H_* \sim \frac{c_{\mathrm{s}*}^2}{H_*} \Rightarrow H_* \sim \frac{c_{\mathrm{s}*}}{\Omega_{\mathrm{K}}(r_*)}, \tag{1.28}$$

where we are comparing the magnitudes of the vertical gravity term and the pressure-gradient term. For thin disk we expect $r_* \gg H_*$ and therefore we can introduce an expansion parameter

$$\epsilon \equiv \frac{H_*}{r_*} \sim \frac{c_{s*}}{r_* \Omega_*} \ll 1. \tag{1.29}$$

We will assume that all the variables with a tilde are of order unity as $\epsilon \to 0$. Note that the typical values only express the orders of magnitude of their respective quantities. We will also write the gradients of the gravitational potential as follows

$$\frac{\partial \psi}{\partial r} = \frac{rGM_*}{\left(r^2+z^2\right)^{3/2}} = \frac{GM_*}{r^2\left(1+(\frac{z}{r})^2\right)^{3/2}}, \tag{1.30}$$

$$\frac{\partial \psi}{\partial z} = \frac{zGM_*}{\left(r^2+z^2\right)^{3/2}} = \frac{zGM_*}{r^3\left(1+(\frac{z}{r})^2\right)^{3/2}}. \tag{1.31}$$

Plugging these new non-dimensional variables into the governing equations and doing a little bit of algebra results in the following non-dimensional equations of motion (Kluźniak and Kita [2000])

$$\begin{aligned}\epsilon^2 \tilde{v}_r \frac{\partial \tilde{v}_r}{\partial \tilde{r}} + \epsilon \tilde{v}_z \frac{\partial \tilde{v}_r}{\partial \tilde{z}} - \tilde{\Omega}^2 \tilde{r} = &-\frac{1}{\tilde{r}^2}\left[1+\epsilon^2\left(\frac{\tilde{z}}{\tilde{r}}\right)^2\right]^{-3/2} - \epsilon^2 n \frac{\partial \tilde{c}_{\rm s}^2}{\partial \tilde{r}} - \epsilon^3\left(\frac{2\tilde{\eta}\tilde{v}_r}{\tilde{\rho}\tilde{r}^2}\right) \\ &+\frac{\epsilon^3}{\tilde{\rho}\tilde{r}}\frac{\partial}{\partial \tilde{r}}\left(2\tilde{\eta}\tilde{r}\frac{\partial \tilde{v}_r}{\partial \tilde{r}}\right) + \frac{\epsilon}{\tilde{\rho}}\frac{\partial}{\partial \tilde{z}}\left(\tilde{\eta}\frac{\partial \tilde{v}_r}{\partial \tilde{z}}\right) + \frac{\epsilon^2}{\tilde{\rho}}\frac{\partial}{\partial \tilde{z}}\left(\tilde{\eta}\frac{\partial \tilde{v}_z}{\partial \tilde{r}}\right) \\ &+\frac{\epsilon^3}{\tilde{\rho}}\frac{\partial}{\partial \tilde{r}}\left[\left(\tilde{\xi}-\frac{2}{3}\tilde{\eta}\right)\left(\frac{1}{\tilde{r}}\frac{\partial}{\partial \tilde{r}}(\tilde{r}\tilde{v}_r)\right)\right] + \frac{\epsilon^2}{\tilde{\rho}}\frac{\partial}{\partial \tilde{r}}\left[\left(\tilde{\xi}-\frac{2}{3}\tilde{\eta}\right)\frac{\partial \tilde{v}_z}{\partial \tilde{z}}\right],\end{aligned} \tag{1.32}$$

$$\epsilon\frac{\tilde{\rho}\tilde{v}_r}{\tilde{r}^2}\left[\frac{\partial}{\partial \tilde{r}}\left(\tilde{r}^2\tilde{\Omega}\right)\right] + \tilde{\rho}\tilde{v}_z\frac{\partial \tilde{\Omega}}{\partial \tilde{z}} = \epsilon^2\left[\frac{1}{\tilde{r}^3}\frac{\partial}{\partial \tilde{r}}\left(\tilde{\eta}\tilde{r}^3\frac{\partial \tilde{\Omega}}{\partial \tilde{r}}\right)\right] + \frac{\partial}{\partial \tilde{z}}\left(\tilde{\eta}\frac{\partial \tilde{\Omega}}{\partial \tilde{z}}\right), \tag{1.33}$$

$$\begin{aligned}\epsilon\tilde{v}_r\frac{\partial \tilde{v}_z}{\partial \tilde{r}} + \tilde{v}_z\frac{\partial \tilde{v}_z}{\partial \tilde{z}} = &-\frac{\tilde{z}}{\tilde{r}^3}\left[1+\epsilon^2\left(\frac{\tilde{z}}{\tilde{r}}\right)^2\right]^{-3/2} - n\frac{\partial \tilde{c}_{\rm s}^2}{\partial \tilde{z}} + \frac{2}{\tilde{\rho}}\frac{\partial}{\partial \tilde{z}}\left(\tilde{\eta}\frac{\partial \tilde{v}_z}{\partial \tilde{z}}\right) \\ &+\frac{\epsilon^2}{\tilde{\rho}\tilde{r}}\frac{\partial}{\partial \tilde{r}}\left(\tilde{\eta}\tilde{r}\frac{\partial \tilde{v}_z}{\partial \tilde{r}}\right) + \frac{\epsilon}{\tilde{\rho}\tilde{r}}\frac{\partial}{\partial \tilde{r}}\left(\tilde{\eta}\tilde{r}\frac{\partial \tilde{v}_r}{\partial \tilde{z}}\right) \\ &+\frac{1}{\tilde{\rho}}\frac{\partial}{\partial \tilde{z}}\left[\left(\tilde{\xi}-\frac{2}{3}\tilde{\eta}\right)\frac{\partial \tilde{v}_z}{\partial \tilde{z}}\right] + \frac{\epsilon}{\tilde{\rho}}\frac{\partial}{\partial \tilde{z}}\left[\left(\tilde{\xi}-\frac{2}{3}\tilde{\eta}\right)\left(\frac{1}{\tilde{r}}\frac{\partial}{\partial \tilde{r}}(\tilde{r}\tilde{v}_r)\right)\right],\end{aligned} \tag{1.34}$$

$$\frac{\epsilon}{\tilde{r}}\frac{\partial}{\partial \tilde{r}}\left(\tilde{r}\tilde{\rho}\tilde{v}_r\right) + \frac{\partial}{\partial \tilde{z}}\left(\tilde{\rho}\tilde{v}_z\right) = 0. \tag{1.35}$$

This is a system of four non-linear partial differential equations for four quantities: $\tilde{v}_r, \tilde{v}_z, \tilde{\Omega}, \tilde{c}_{\rm s}$. The values of other variables $\tilde{\rho}, \tilde{\nu}, \tilde{P}, \tilde{\eta}, \dot{M}$ follow from these four. The first three quantities give us the velocity field, and the fourth one is the speed of sound, from which all the thermodynamic quantities follow. We

will solve these equations by expanding all the quantities into a power series of ϵ and then solving the equations separately for each power of ϵ. We will use our two constants of integration as a shortcut to solve for the disk semi-thickness $\tilde{H}(\tilde{r})$. The constants of integration bring no new information to the equations - we could solve for $\tilde{H}$ even if we did not know these constants, but it would be more difficult.

Our assumption of equatorial plane symmetry implies that we assume the functions $\Omega, v_r, c_\mathrm{s}, \rho, \eta, P$ to be even functions of the z coordinate. This means that all of these quantities with a tilde must also be even functions of $\tilde{z}$, since the scaling does not break the symmetry. However, the vertical velocity v_z has to be an odd function of $\tilde{z}$. We will therefore assume all the terms in the power expansion of given variables to be either odd for v_z or even for the rest.

2. Outer disk solution

In this chapter, we still follow KK very closely. We start with the outer disk because it will give us information on how to rescale our quantities into the boundary layer. We find the lowest order solution to the Navier-Stokes equation and the second order correction of the azimuthal frequency. We will also be able to calculate the disk semi-thickness with the information acquired. This will lead us to a singularity at a specific radius $\tilde{r}_+$, which will be defined later.

2.1 Zeroth-order solution

Let us now solve the equations with the strategy described above. We will denote each order of the given quantity with the corresponding number of the order of the expansion parameter ϵ. We start by writing out the equations in the lowest order (ϵ^0) as (Kluźniak and Kita [2000])

$$-\tilde{\Omega}_0^2 \tilde{r} = -\frac{1}{\tilde{r}^2}, \tag{2.1}$$

$$\tilde{\rho}_0 \tilde{v}_{z0} \frac{\partial \tilde{\Omega}_0}{\partial \tilde{z}} = \frac{\partial}{\partial \tilde{z}} \left(\tilde{\eta}_0 \frac{\partial \tilde{\Omega}_0}{\partial \tilde{z}} \right), \tag{2.2}$$

$$\tilde{v}_{z0} \frac{\partial \tilde{v}_{z0}}{\partial \tilde{z}} = -\frac{\tilde{z}}{\tilde{r}^3} - n \frac{\partial \tilde{c}_{s0}^2}{\partial \tilde{z}} + \frac{2}{\tilde{\rho}_0} \frac{\partial}{\partial \tilde{z}} \left(\tilde{\eta}_0 \frac{\partial \tilde{v}_{z0}}{\partial \tilde{z}} \right) + \frac{1}{\tilde{\rho}_0} \frac{\partial}{\partial \tilde{z}} \left[\left(\tilde{\xi}_0 - \frac{2}{3} \tilde{\eta}_0 \right) \frac{\partial \tilde{v}_{z0}}{\partial \tilde{z}} \right], \tag{2.3}$$

$$\frac{\partial}{\partial \tilde{z}} \left(\tilde{\rho}_0 \tilde{v}_{z0} \right) = 0. \tag{2.4}$$

Looking at equation (2.1), we immediately get explicit formula for $\tilde{\Omega}_0$

$$\tilde{\Omega}_0 = \frac{1}{\tilde{r}^{3/2}}, \tag{2.5}$$

which is the dimensionless version of the Keplerian azimuthal frequency Ω_{K}. Plugging this result into equation (2.2) gives $0 = 0$ since $\tilde{\Omega}_0$ is not a function of $\tilde{z}$. If we continue examining the equations one by one, equation (2.3) might look daunting, so we will first examine the continuity equation (2.4). We will integrate this equation with respect to $\tilde{z}$ giving us

$$\tilde{\rho}_0 \tilde{v}_{z0} = f(\tilde{r}), \tag{2.6}$$

where $f(\tilde{r})$ is constant in $\tilde{z}$, which means it is an even function of $\tilde{z}$. We will now compare both sides' parity. Since $\tilde{\rho}$ is an even function of $\tilde{z}$ and $\tilde{v}_{z0}$ has to be an odd function of $\tilde{z}$, the left-hand side of this equation is an odd function of $\tilde{z}$. This equation can only be satisfied if $\tilde{v}_{z0} = 0 = f(\tilde{r})$. Let us now use this result in solving the remaining equation. Plugging in our results, the vertical equation (2.3) simplifies into

$$0 = -\frac{\tilde{z}}{\tilde{r}^3} - \frac{3}{2} \frac{\partial \tilde{c}_{s0}^2}{\partial \tilde{z}}. \tag{2.7}$$

We can solve this equation by integration with respect to $\tilde{z}$ yielding

$$\tilde{c}_{\mathrm{s}0}^2 = -\frac{z^2}{3r^3} + \kappa(\tilde{r}), \tag{2.8}$$

where κ is a constant of integration. However, κ can be a function of $\tilde{r}$. It is necessary for the speed of sound to be zero outside of the disk, since $c_{\mathrm{s}} = 0 \Leftrightarrow \rho = 0$. Thus, we choose κ such that

$$\tilde{c}_{\mathrm{s}0}^2 = \frac{\tilde{\Omega}_0^2}{3}\left(\tilde{H}_0^2 - \tilde{z}^2\right), \tag{2.9}$$

where $\tilde{H}_0$ is the zeroth order semi-thickness of the disk. Let us now consider equation for the pressure gradient in the $\tilde{z}$ direction (1.5). Using equation (2.7) we can write

$$-\frac{\tilde{z}}{\tilde{r}^3} = \frac{3}{2}\frac{\partial \tilde{c}_{\mathrm{s}0}^2}{\partial \tilde{z}} = \frac{1}{\tilde{\rho}_0}\frac{\partial \tilde{P}_0}{\partial \tilde{z}}. \tag{2.10}$$

We will use the first term and the last term in calculating P_0. Since we know the relation between the speed of sound, pressure and density given by equation (1.4) and we know the polytropic equation, we can calculate the pressure and density. We calculate with polytropic index $n = 3/2$ as follows

$$\tilde{c}_{\mathrm{s}0}^2 = \left(\frac{n+1}{n}\right)\frac{\tilde{P}_0}{\tilde{\rho}_0} = \left(\frac{n+1}{n}\right)\tilde{\rho}_0^{\frac{1}{n}} \Rightarrow \tilde{\rho}_0 = \left(\frac{\tilde{\Omega}_0^2}{5}\left(\tilde{H}_0^2 - \tilde{z}^2\right)\right)^{3/2}, \tag{2.11}$$

$$\tilde{P}_0 = \tilde{\rho}^{\frac{n+1}{n}} = \left(\frac{\tilde{\Omega}_0^2}{5}\left(\tilde{H}_0^2 - \tilde{z}^2\right)\right)^{5/2}. \tag{2.12}$$

We should note that both $\tilde{P}_0$ and $\tilde{\rho}_0$ are functions of both $\tilde{z}$ and $\tilde{r}$, since $\tilde{H}_0$ is a function of $\tilde{r}$. We obtained the same functional dependence as Hōshi [1977]. We will now use our assumption of ν to be height dependant, with a constant α, similar to how KK do it in their paper.[1] We will write the kinematic viscosity as (Umurhan et al. [2006])

$$\nu = \frac{2}{3}\frac{\alpha}{\Omega_{\mathrm{K}}}\frac{c_{\mathrm{s}}^2}{(1+1/n)} = \frac{2}{5}\frac{\alpha c_{\mathrm{s}}^2}{\Omega_{\mathrm{K}}}. \tag{2.13}$$

We can then write the dynamic viscosity in the zeroth order as

$$\tilde{\eta}_0 = \tilde{\nu}_0\tilde{\rho}_0 = \frac{2\alpha}{3\tilde{\Omega}_0}\left(\frac{\tilde{\Omega}_0^2}{5}\left(\tilde{H}_0^2 - \tilde{z}^2\right)\right)^{5/2}. \tag{2.14}$$

2.2 First-order solution

We keep the previous results in mind, and we write the equations for the first order terms. We get the following equations

$$\tilde{v}_{z0}\frac{\partial \tilde{v}_{r0}}{\partial \tilde{z}} - 2\tilde{\Omega}_0\tilde{\Omega}_1\tilde{r} = \frac{1}{\tilde{\rho}_0}\frac{\partial}{\partial \tilde{z}}\left(\tilde{\eta}_0\frac{\partial \tilde{v}_{r0}}{\partial \tilde{z}}\right), \tag{2.15}$$

[1] Note: there is a typo in Kluźniak and Kita [2000] - missing factor 2/3 in their definition of ν.

$$\frac{\tilde{\rho}_0\tilde{v}_{r0}}{\tilde{r}^2}\left[\frac{\partial\left(\tilde{r}^2\tilde{\Omega}_0\right)}{\partial\tilde{r}}\right]+\tilde{\rho}_0\tilde{v}_{z0}\frac{\partial\tilde{\Omega}_1}{\partial\tilde{z}}+\tilde{\rho}_0\tilde{v}_{z1}\frac{\partial\tilde{\Omega}_0}{\partial\tilde{z}}=\frac{\partial}{\partial\tilde{z}}\left(\tilde{\eta}\frac{\partial\tilde{\Omega}_1}{\partial\tilde{z}}\right), \tag{2.16}$$

$$\begin{aligned}\tilde{v}_{r0}\frac{\partial\tilde{v}_{z0}}{\partial\tilde{r}}+\tilde{v}_{z1}\frac{\partial\tilde{v}_{z0}}{\partial\tilde{z}}+\tilde{v}_{z0}\frac{\partial\tilde{v}_{z1}}{\partial\tilde{z}}=-3\frac{\partial\tilde{c}_{\mathrm{s}0}\tilde{c}_{\mathrm{s}1}}{\partial\tilde{z}}+\frac{2}{\tilde{\rho}_0}\frac{\partial}{\partial\tilde{z}}\left(\tilde{\eta}_0\frac{\partial\tilde{v}_{z1}}{\partial\tilde{z}}\right)\\+\frac{1}{\tilde{\rho}_0\tilde{r}}\frac{\partial}{\partial\tilde{r}}\left(\tilde{\eta}_0\tilde{r}\frac{\partial\tilde{v}_{r0}}{\partial\tilde{z}}\right)+\frac{1}{\tilde{\rho}_0}\frac{\partial}{\partial\tilde{z}}\left[\left(\tilde{\xi}_0-\frac{2}{3}\tilde{\eta}_0\right)\left(\frac{1}{\tilde{r}}\frac{\partial(\tilde{r}\tilde{v}_{r0})}{\partial\tilde{r}}+\frac{\partial\tilde{v}_{z1}}{\partial\tilde{z}}\right)\right],\end{aligned} \tag{2.17}$$

$$\frac{1}{\tilde{r}}\frac{\partial}{\partial\tilde{r}}\left(\tilde{r}\tilde{\rho}_0\tilde{v}_{r0}\right)+\frac{\partial}{\partial\tilde{z}}\left(\tilde{\rho}_0\tilde{v}_{z1}\right)=0. \tag{2.18}$$

These equations significantly simplify if we use the results from the zeroth order. It is at this point where KK argue that the symmetry of Ω_1 implies $\Omega_1 = 0$. However, it is not obvious to us. If we were to write these equations explicitly, we would find that symmetry does not seem play any role in them. Equations (2.15) and (2.16) become linear differential equations for $\tilde{v}_{r0}$ and $\tilde{\Omega}_1$. We can plug for either of these quantities from one equation into the other and obtain a single linear differential equation of fourth order, whose solution would likely be a polynomial. However, the right-hand side of this equation would be zero; hence we do not have any reason not to choose the trivial solution. Here we also assume that there are no boundary conditions that the trivial solution would not meet. We thus set $\tilde{v}_{r0} = \tilde{\Omega}_1 = 0$. Plugging $\tilde{v}_{r0} = 0$ into the continuity equation (2.18) and using the same argument we did when calculating $\tilde{v}_{z0}$, we get that $\tilde{v}_{z1} = 0$. With these results, the only surviving term in the vertical equation (2.17) is the first term on the right-hand side. From this, it follows that $\tilde{c}_{\mathrm{s}1} = 0$. The speed of sound being equal to zero in the first order implies $\tilde{P}_1 = 0$ and $\tilde{\rho}_1 = 0$. With the first-order results, we can now compute the disk thickness.

2.3 Disk thickness

We have yet to rescale our constant of integration obtained in Section 1.3, so let us do that now. Using our scalings discussed in Section 1.4, we can rewrite equation (1.18) as

$$\dot{M} = -2\pi\tilde{r}r_*\int_{-\infty}^{\infty}\tilde{\rho}\rho_* c_{\mathrm{s}*}\tilde{v}_r H_*\mathrm{d}\tilde{z}. \tag{2.19}$$

Dividing both sides by the typical values on the right-hand side, one can write

$$\frac{\dot{M}}{2\pi r_*\rho_* c_{\mathrm{s}*}H_*} = \epsilon\frac{\dot{M}}{2\pi\rho_* c_{\mathrm{s}*}H_*^2} = -\tilde{r}\int_{-\infty}^{\infty}\tilde{\rho}\tilde{v}_r\mathrm{d}\tilde{z}. \tag{2.20}$$

We will introduce a dimensionless constant $\dot{m}$ as

$$\dot{m} = \frac{\dot{M}}{2\pi\rho_* c_{\mathrm{s}*}H_*^2}, \tag{2.21}$$

whose order is at the moment unknown. We do know that $\dot{m}$ is at lowest of order unity as the right-hand side is at least $O(\epsilon)$ as $\tilde{v}_{r0}$ is zero. We will later show

that $\tilde{v}_{r1}$ is not zero, hence $\dot{m}$ is $O(1)$. This allows us to rewrite equation (2.19) in terms of $\dot{m}$

$$\epsilon\dot{m} = -\tilde{r}\int_{-\infty}^{\infty}\tilde{\rho}\tilde{v}_r \mathrm{d}\tilde{z}. \tag{2.22}$$

If we use the expansion of $\tilde{\rho}$ and $\tilde{v}_r$, we get in the lowest non-zero order

$$\dot{m} = -\tilde{r}\int_{-\tilde{H}_0}^{\tilde{H}_0}\tilde{\rho}_0\tilde{v}_{r1}\mathrm{d}\tilde{z} - \tilde{r}\int_{-\tilde{H}_0}^{\tilde{H}_0}\tilde{\rho}_1\tilde{v}_{r0}\mathrm{d}\tilde{z}, \tag{2.23}$$

where the second term is identically zero from the results we have obtained thus far. However, we cannot calculate the first term at the moment since we have no results for $\tilde{v}_{r1}$ yet. Let us now rescale the second constant of integration defined by equation (1.27). We will use the fact that $\tilde{\Omega}$ is independent of $\tilde{z}$ in the lowest order and hence we write

$$\dot{M}\left(j_{\mathrm{K}} - j_{+}\right) = -2\pi\tilde{r}^3 r_*^3\int_{-\infty}^{\infty} c_{\mathrm{s}*}H_*\rho_*\tilde{\eta}\frac{\partial\tilde{\Omega}}{\partial\tilde{r}}\frac{\Omega_*}{r_*}H_*\mathrm{d}\tilde{z}, \tag{2.24}$$

where we denoted $\langle j\rangle$ as j_{K}, since we know that the angular frequency Ω behaves in a Keplerian manner in the outer region and is therefore independent of $\tilde{z}$. We will now rescale the angular momenta as well since we know that $j = \Omega r^2$, and we divide both sides by the constants on the right-hand side of equation (2.24). We obtain

$$\frac{\dot{M}}{2\pi\rho_* c_{\mathrm{s}*}H_*^2}\left(\tilde{j}_{\mathrm{K}} - \tilde{j}_{+}\right) = -\tilde{r}^3\int_{-\infty}^{\infty}\tilde{\eta}\frac{\partial\tilde{\Omega}}{\partial\tilde{r}}\mathrm{d}\tilde{z}, \tag{2.25}$$

where we denoted the rescaled angular momenta as $\tilde{j}_{\mathrm{K}}$ and $\tilde{j}_{+}$, which are again $O(1)$. We also assume that $\tilde{j}_{+}$ is the Keplerian angular momentum at a certain radius $\tilde{r}_{+}$. Using our definition of $\dot{m}$, we can rewrite this equation as

$$\dot{m}\left(\tilde{j}_{\mathrm{K}} - \tilde{j}_{+}\right) = -\tilde{r}^3\int_{-\infty}^{\infty}\tilde{\eta}\frac{\partial\tilde{\Omega}}{\partial\tilde{r}}\mathrm{d}\tilde{z}. \tag{2.26}$$

The left-hand side is clearly of order unity, hence we plug into the right-hand side our zeroth-order results giving us

$$\dot{m}\left(\tilde{j}_{\mathrm{K}} - \tilde{j}_{+}\right) = -\tilde{r}^3\frac{\mathrm{d}\tilde{\Omega}_0}{\mathrm{d}\tilde{r}}\int_{-\tilde{H}_0}^{\tilde{H}_0}\tilde{\eta}_0\mathrm{d}\tilde{z}. \tag{2.27}$$

We can write the derivate of $\tilde{\Omega}_0$ in front of the integral as it does not depend on the vertical coordinate. We can now plug in our results and calculate the integral. Let us first look at what function we are integrating. The only dependence of $\tilde{\eta}_0$ on $\tilde{z}$ takes the form of $\left(\tilde{H}_0^2 - \tilde{z}^2\right)^{5/2}$, which is the only part we need to integrate. Let us now calculate the integral

$$\int_{-\tilde{H}_0}^{\tilde{H}_0}\left(\tilde{H}_0^2 - \tilde{z}^2\right)^{5/2}\mathrm{d}\tilde{z} = \frac{5\pi}{16}\tilde{H}_0^6. \tag{2.28}$$

We will now plug this result into equation (2.27) and calculate for $\tilde{H}_0$, yielding the disk semi-thickness in the lowest order (Kluźniak and Kita [2000])

$$\tilde{H}_0 = \left[\frac{16\tilde{r}^{\frac{11}{2}}5^{\frac{3}{2}}\dot{m}}{\pi\alpha}\left(\tilde{r}^{\frac{1}{2}} - \tilde{r}_{+}^{\frac{1}{2}}\right)\right]^{\frac{1}{6}}. \tag{2.29}$$

We see that $\tilde{H}_0$ goes to zero at $\tilde{r}_+$. Although we do not have an exact formula for $\dot{m}$ yet, it does not matter as it is a constant in both $\tilde{r}$ and $\tilde{z}$, so our functional dependence of $\tilde{r}$ is independent of whatever $\dot{m}$ may be. This prescription for $\tilde{H}$ leads to singular behaviour of the lowest non-zero orders of the vertical and radial velocities as well as the second order correction to the Keplerian azimuthal frequency. This is caused by the assumption that $\tilde{\Omega} \sim \tilde{\Omega}_{\mathrm{K}}$ in the neighbourhood of $\tilde{r}_+$, which is not true.

In real flow, the corrections to the Keplerian angular frequency $\tilde{\Omega}_{\mathrm{K}}$ and their radial gradients become important in the vicinity of the zero-torque radius $\tilde{r}_+$. This makes the radial gradient of the angular frequency $\partial\tilde{\Omega}/\partial\tilde{r}$ in equation (2.26) to vanish at $\tilde{r}_+$. This equation is then satisfied without the need for the disk semi-thickness to go to zero. The pattern of the flow around r_+ changes much faster in the radial direction than in the outer disk and a boundary layer is created. In the case of neutron-star accretion disks, the boundary layers appear as a consequence of the inner boundary condition at the surface of the star. When the rotation of the star is slower than the Keplerian angular frequency at the stellar radius, the rotation of the flow has to decelerate to match the rotation of the star. The zeroth-order approximation found in Section 2.1 describes the accretion flow with Keplerian azimuthal frequency. This stops being a good approximation of the solution in a narrow region, where the solution rapidly changes its nature in order to satisfy the boundary condition on the stellar surface. Some ideas how to describe the boundary layers using singular perturbation methods will be provided in Chapter 3.

2.4 Second-order solution

In this section, we look at the second order disk equations as they are the ones which describe the backflows in the disk, and also the divergent terms are found from the second order equations. We solve them using an ansatz since these equations will not have as simple solutions as the zeroth and first orders. In this section, our approach will slightly differ from KK. Nevertheless, we obtain the same results. The governing equations in the second order are (Kluźniak and Kita [2000])

$$-2\tilde{\Omega}_0\tilde{\Omega}_2 r = \frac{3}{2\tilde{r}^2}\left(\frac{\tilde{z}}{\tilde{r}}\right)^2 - \frac{3}{2}\frac{\partial\tilde{c}_{\mathrm{s}0}^2}{\partial\tilde{r}} + \frac{1}{\tilde{\rho}_0}\frac{\partial}{\partial\tilde{z}}\left(\tilde{\eta}_0\frac{\partial\tilde{v}_{r1}}{\partial\tilde{z}}\right), \tag{2.30}$$

$$\frac{\tilde{\rho}_0\tilde{v}_{r1}}{\tilde{r}^2}\left[\frac{\mathrm{d}}{\mathrm{d}\tilde{r}}\left(\tilde{r}^2\tilde{\Omega}_0\right)\right] = \frac{1}{\tilde{r}^3}\frac{\partial}{\partial\tilde{r}}\left(\tilde{\eta}_0\tilde{r}^3\frac{\mathrm{d}\tilde{\Omega}_0}{\mathrm{d}\tilde{r}}\right) + \frac{\partial}{\partial\tilde{z}}\left(\tilde{\eta}_0\frac{\partial\tilde{\Omega}_2}{\partial\tilde{z}}\right), \tag{2.31}$$

$$\begin{aligned} 0 = \frac{3}{2}\frac{\tilde{z}^3}{\tilde{r}^5} - 3\frac{\partial(\tilde{c}_{\mathrm{s}0}\tilde{c}_{\mathrm{s}2})}{\partial\tilde{z}} + \frac{2}{\tilde{\rho}_0}\frac{\partial}{\partial\tilde{z}}\left(\tilde{\eta}_0\frac{\partial\tilde{v}_{z2}}{\partial\tilde{z}}\right) + \frac{1}{\tilde{\rho}_0}\frac{\partial}{\partial\tilde{z}}\left[\left(\tilde{\xi}_0 - \frac{2}{3}\tilde{\eta}_0\right)\frac{\partial\tilde{v}_{z2}}{\partial\tilde{z}}\right] \\ + \frac{1}{\tilde{\rho}_0}\frac{\partial}{\partial\tilde{z}}\left[\left(\tilde{\xi}_0 - \frac{2}{3}\tilde{\eta}_0\right)\left(\frac{1}{\tilde{r}}\frac{\partial}{\partial\tilde{r}}(\tilde{r}\tilde{v}_{r1})\right)\right], \end{aligned} \tag{2.32}$$

$$\frac{1}{\tilde{r}}\frac{\partial}{\partial\tilde{r}}\left(\tilde{r}\tilde{\rho}_0\tilde{v}_{r1}\right) + \frac{\partial}{\partial\tilde{z}}\left(\tilde{\rho}_0\tilde{v}_{z2}\right) = 0. \tag{2.33}$$

Now it is assumed in KK's paper that the following ansatz can be made: $\tilde{v}_{r1} = f_0(\tilde{r})(\tilde{H}_0^2 - \tilde{z}^2) + f_2(\tilde{r})$, where we need to find f_0 and f_2. Analogically for $\tilde{\Omega}_2$ and $\tilde{v}_{z2}$. We will, however, try a different approach. We assume, with respect to given symmetries of the quantities, the following: $\tilde{v}_{r1} = A_0(\tilde{r}) + \tilde{z}^2 A_2(\tilde{r}); \tilde{\Omega}_2 = W_0(\tilde{r}) + \tilde{z}^2 W_2(\tilde{r}); \tilde{v}_{z2} = \tilde{z}\left[B_0(\tilde{r}) + \tilde{z}^2 B_2(\tilde{r})\right]$. Before we start solving the equations, let us write a list of some useful equalities:

$$\tilde{\nu} = \frac{\tilde{\eta}}{\tilde{\rho}} = \frac{2}{15}\alpha\tilde{\Omega}_0\left(\tilde{H}_0^2 - \tilde{z}^2\right),$$

$$\tilde{\eta} = \tilde{\nu}\tilde{\rho} = \frac{2\alpha\tilde{P}}{3\tilde{\Omega}_0},$$

$$\frac{\partial\tilde{c}_{s0}^2}{\partial\tilde{r}} = -\frac{\tilde{H}_0^2 - \tilde{z}^2}{\tilde{r}^4} + \frac{2\tilde{H}_0\tilde{H}_0'}{3\tilde{r}^3},$$

$$\frac{\partial\tilde{c}_{s0}^2}{\partial\tilde{z}} = -\frac{2\tilde{\Omega}_0^2\tilde{z}}{3},$$

$$\frac{1}{\tilde{\rho}}\frac{\partial\tilde{\eta}}{\partial\tilde{r}} = \frac{\alpha}{\tilde{\Omega}_0}\left(-\frac{\tilde{H}_0^2 - \tilde{z}^2}{\tilde{r}^4} + \frac{2\tilde{H}_0\tilde{H}_0'}{3\tilde{r}^3}\right) + \frac{\alpha\tilde{\Omega}_0}{5\tilde{r}}\left(\tilde{H}_0^2 - \tilde{z}^2\right),$$

$$\frac{1}{\tilde{\rho}}\frac{\partial\tilde{\eta}}{\partial\tilde{z}} = -\frac{2}{3}\alpha\tilde{\Omega}_0\tilde{z},$$

$$\frac{\partial\tilde{\rho}_0}{\partial\tilde{r}} = 3\frac{\tilde{\Omega}_0^2\tilde{\Omega}_0'}{5^{3/2}}\left(\tilde{H}_0^2 - \tilde{z}^2\right)^{3/2} + 3\frac{\tilde{\Omega}_0^3}{5^{3/2}}\tilde{H}_0\tilde{H}_0'\left(\tilde{H}_0^2 - \tilde{z}^2\right)^{1/2},$$

$$\frac{\partial\tilde{\rho}_0}{\partial\tilde{z}} = -3\tilde{z}\frac{\tilde{\Omega}_0^3}{5^{3/2}}\left(\tilde{H}_0^2 - \tilde{z}^2\right)^{1/2}.$$

We will start with the radial equation (2.30). We plug in our ansatz into the equation, and we write

$$-2\tilde{\Omega}_0(W_0 + \tilde{z}^2 W_2)\tilde{r} = \frac{3\tilde{z}^2}{2\tilde{r}^4} - \frac{3}{2}\left(-\frac{\tilde{H}_0^2 - \tilde{z}^2}{r^4} + \frac{2\tilde{H}_0\tilde{H}_0'}{3\tilde{r}^3}\right) + \frac{4\tilde{z}A_2}{3\tilde{\rho}_0}\frac{\partial\tilde{\eta}_0}{\partial\tilde{z}} + \frac{4A_2\tilde{\eta}_0}{3\tilde{\rho}_0}. \tag{2.34}$$

Using our list of identities, this equation simplifies into

$$\begin{aligned}-2\tilde{\Omega}_0(W_0 + \tilde{z}^2 W_2)\tilde{r} = \frac{3}{2\tilde{r}^2}\frac{\tilde{z}^2}{\tilde{r}^2} - \frac{3}{2}\left(-\frac{\tilde{H}_0^2 - \tilde{z}^2}{r^4} + \frac{2\tilde{H}_0\tilde{H}_0'}{3\tilde{r}^3}\right)\\ -\frac{4\tilde{z}^2}{3}A_2\tilde{\Omega}_0\alpha + \frac{4}{15}A_2\alpha\tilde{\Omega}_0(\tilde{H}_0^2 - \tilde{z}^2).\end{aligned} \tag{2.35}$$

We can now separate for each order of $\tilde{z}$ and obtain two equations. For $\tilde{z}^0$ we write:

$$-2\tilde{\Omega}_0 W_0\tilde{r} = \frac{3\tilde{H}_0^2}{2r^4} - \frac{\tilde{H}_0\tilde{H}_0'}{\tilde{r}^3} + \frac{4}{15}A_2\alpha\tilde{\Omega}_0\tilde{H}_0^2. \tag{2.36}$$

And for $\tilde{z}^2$ we get

$$-2\tilde{\Omega}_0 W_2\tilde{r} = \frac{3}{2\tilde{r}^4} - \frac{3}{2\tilde{r}^4} - \frac{4}{3}A_2\tilde{\Omega}_0\alpha - \frac{4A_2\alpha\Omega_0}{15}, \tag{2.37}$$

which yields

$$W_2 = \frac{4A_2\alpha}{5\tilde{r}}. \tag{2.38}$$

Let us now have a look at the azimuthal equation (2.31). We first divide the equation by the density $\tilde{\rho}$. We can write

$$\tilde{r}\left(A_0 + \tilde{z}^2 A_2\right)\frac{\mathrm{d}\tilde{r}^{1/2}}{\mathrm{d}\tilde{r}} = \frac{\tilde{r}^3\tilde{\Omega}_0'}{\tilde{\rho}_0}\frac{\partial\tilde{\eta}_0}{\partial\tilde{r}} + \frac{\tilde{\eta}_0}{\tilde{\rho}_0}\frac{\mathrm{d}}{\mathrm{d}\tilde{r}}\left(\tilde{r}^3\tilde{\Omega}_0'\right) + \frac{2\tilde{z}W_2\tilde{r}^3}{\tilde{\rho}_0}\frac{\partial\tilde{\eta}_0}{\partial\tilde{z}} + 2W_2\tilde{r}^3\frac{\tilde{\eta}_0}{\tilde{\rho}_0}, \tag{2.39}$$

which after plugging in our equalities becomes:

$$\begin{aligned}\tilde{r}\left(A_0 + \tilde{z}^2 A_2\right)\frac{\mathrm{d}\tilde{r}^{1/2}}{\mathrm{d}\tilde{r}} = \tilde{r}^3\tilde{\Omega}_0'\left[\frac{\alpha}{\tilde{\Omega}_0}\left(-\frac{\tilde{H}_0^2 - \tilde{z}^2}{\tilde{r}^4} + \frac{2\tilde{H}_0\tilde{H}_0'}{3\tilde{r}^3}\right) + \frac{\alpha\tilde{\Omega}_0}{5\tilde{r}}\left(\tilde{H}_0^2 - \tilde{z}^2\right)\right] \\ + \frac{2}{15}\alpha\tilde{\Omega}_0\left(\tilde{H}_0^2 - \tilde{z}^2\right)\frac{\mathrm{d}}{\mathrm{d}\tilde{r}}\left(\tilde{r}^3\tilde{\Omega}_0'\right) - \frac{4}{3}\tilde{z}^2 W_2\tilde{r}^3\tilde{\Omega}_0\alpha + \frac{4}{15}W_2\tilde{r}^3\alpha\tilde{\Omega}_0\left(\tilde{H}_0^2 - \tilde{z}^2\right).\end{aligned} \tag{2.40}$$

We have not yet simplified this equation, so that it is a bit clearer as to how we got this equation. We will simplify the equation now, when we separate for each order of $\tilde{z}$. For $\tilde{z}^0$ we get

$$\begin{aligned}\frac{\sqrt{\tilde{r}}}{2}A_0 = -\frac{3}{2}\tilde{r}^2\tilde{\Omega}_0\left[\frac{\alpha}{\tilde{\Omega}_0}\left(-\frac{\tilde{H}_0^2}{\tilde{r}^4} + \frac{2\tilde{H}_0\tilde{H}_0'}{3\tilde{r}^3}\right) + \frac{\alpha\tilde{\Omega}_0}{5\tilde{r}}\tilde{H}_0^2\right] \\ - \frac{\alpha\tilde{\Omega}_0}{10\sqrt{\tilde{r}}}\tilde{H}_0^2 + \frac{4}{15}\tilde{r}^3 W_2\alpha\tilde{\Omega}_0\tilde{H}_0^2.\end{aligned} \tag{2.41}$$

And for $\tilde{z}^2$ we write

$$\frac{\sqrt{\tilde{r}}}{2}A_2 = -\frac{3}{2}\tilde{r}^2\tilde{\Omega}_0\left[\frac{\alpha}{\tilde{\Omega}_0\tilde{r}^4} - \frac{\alpha\tilde{\Omega}_0}{5\tilde{r}}\right] + \frac{\alpha\tilde{\Omega}_0}{10\sqrt{\tilde{r}}} - \frac{4}{3}\tilde{r}^3 W_2\alpha\tilde{\Omega}_0 - \frac{4}{15}\tilde{r}^3 W_2\alpha\tilde{\Omega}_0. \tag{2.42}$$

We will now use equation (2.38) to plug in for A_2 into equation (2.42). Simplifying, we can write

$$\frac{5\tilde{r}^{3/2}}{8\alpha}W_2 = -\frac{11\alpha}{10\tilde{r}^2} - \frac{24}{15}\alpha\tilde{\Omega}_0\tilde{r}^3 W_2. \tag{2.43}$$

Solving for W_2 we get

$$W_2 = -\frac{\alpha^2}{\tilde{r}^{7/2}}\frac{44}{25 + 64\alpha^2}. \tag{2.44}$$

Let us now introduce constant factor Λ, which may come in handy when comparing our results to the results of KK,

$$\Lambda = \frac{11}{5}\frac{1}{1 + \frac{64}{25}\alpha^2}. \tag{2.45}$$

We can rewrite W_2 using Λ as follows

$$W_2 = -\frac{4}{5}\frac{\Lambda\alpha^2}{\tilde{r}^{7/2}}. \tag{2.46}$$

With the knowledge of W_2, we can calculate A_2. We will now use equation (2.36) to get W_0. We write

$$-2\tilde{\Omega}_0 W_0 \tilde{r} = \frac{\tilde{H}_0^2}{\tilde{r}^4}\left(\frac{3}{2} - \frac{\tilde{H}_0'}{\tilde{H}_0}\tilde{r} + \frac{4}{15}A_2\alpha\tilde{\Omega}_0\tilde{r}^4\right), \tag{2.47}$$

which after plugging in for A_2 and further simplifying yields

$$W_0 = \frac{\tilde{H}_0^2}{\tilde{r}^{7/2}}\left(-\frac{3}{4} + \frac{1}{2}\frac{\mathrm{d}\ln\tilde{H}_0}{\mathrm{d}\ln\tilde{r}} + \frac{2}{15}\alpha^2\Lambda\right). \tag{2.48}$$

We have thus obtained a second-order correction for Ω, which is in agreement with KK. For completeness, we write out the result:

$$\Omega_2 = \frac{\tilde{H}_0^2}{\tilde{r}^{7/2}}\left[-\frac{3}{4} + \frac{1}{2}\frac{\mathrm{d}\ln\tilde{H}_0}{\mathrm{d}\ln\tilde{r}} + \frac{2}{15}\alpha^2\Lambda\left(1 - 6\frac{\tilde{z}^2}{\tilde{H}_0^2}\right)\right]. \tag{2.49}$$

We have yet to solve for A_0. For this we will use equation (2.41) as follows

$$A_0 = -\frac{3\alpha}{\tilde{\Omega}_0}\left(-\frac{\tilde{H}_0^2}{\tilde{r}^4} + \frac{2\tilde{H}_0\tilde{H}_0'}{3\tilde{r}^3}\right) - \frac{4\alpha\tilde{\Omega}_0}{5\tilde{r}}\tilde{H}_0^2 + \frac{8}{15}\tilde{r}\alpha W_2\tilde{H}_0^2. \tag{2.50}$$

Simplifying leads to

$$A_0 = \frac{\alpha\tilde{H}_0^2}{\tilde{r}^{5/2}}\left(\frac{11}{5} - 2\frac{\mathrm{d}\ln\tilde{H}_0}{\mathrm{d}\ln\tilde{r}} - \frac{32}{75}\alpha^2\Lambda\right). \tag{2.51}$$

Therefore, we got the same result as KK. One can check for themselves, that for $\tilde{v}_{r1}$ we can write

$$\tilde{v}_{r1} = \alpha\frac{\tilde{H}_0^2}{\tilde{r}^{5/2}}\left[\Lambda\left(1 - \frac{\tilde{z}^2}{\tilde{H}_0^2}\right) + \frac{32}{15}\Lambda\alpha^2 - 2\frac{\mathrm{d}\ln\tilde{H}_0}{\mathrm{d}\ln\tilde{r}}\right]. \tag{2.52}$$

We will now inspect the continuity equation (2.33). We plug in our ansatz while also taking the derivatives. We write

$$\begin{aligned}\left(A_0 + \tilde{z}^2A_2\right)\frac{\partial\tilde{\rho}_0}{\partial\tilde{r}} + \tilde{\rho}_0\left(A_0' + \tilde{z}^2A_2'\right) + \frac{\tilde{\rho}_0}{\tilde{r}}\left(A_0 + \tilde{z}^2A_2\right)\\ + \left(\tilde{z}B_0 + \tilde{z}^3B_2\right)\frac{\partial\tilde{\rho}_0}{\partial\tilde{z}} + \tilde{\rho}_0\left(B_0 + 3\tilde{z}^2B_2\right) = 0,\end{aligned} \tag{2.53}$$

which after plugging in for $\tilde{\rho}_0$ yields

$$\begin{aligned}&\left(A_0 + \tilde{z}^2A_2\right)\left[-\frac{7}{2}\frac{\tilde{\Omega}_0^3}{5^{3/2}\tilde{r}}\left(\tilde{H}_0^2 - \tilde{z}^2\right)^{3/2} + \frac{3\tilde{H}_0'\tilde{H}_0\tilde{\Omega}_0^3}{5^{3/2}}\left(\tilde{H}_0^2 - \tilde{z}^2\right)^{1/2}\right]\\ &+\left(A_0' + \tilde{z}^2A_2'\right)\frac{\tilde{\Omega}_0^3}{5^{3/2}}\left(\tilde{H}_0^2 - \tilde{z}^2\right)^{3/2} - \left(\tilde{z}^2B_0 + \tilde{z}^4B_2\right)\frac{3\tilde{\Omega}_0^3}{5^{3/2}}\left(\tilde{H}_0^2 - \tilde{z}^2\right)^{1/2}\\ &+\frac{\tilde{\Omega}_0^3}{5^{3/2}}\left(\tilde{H}_0^2 - \tilde{z}^2\right)^{3/2}\left(B_0 + 3\tilde{z}^2B_2\right) = 0.\end{aligned} \tag{2.54}$$

We divide this equation by $\left(\Omega_0^3/5^{3/2}\right)\left(\tilde{H}_0^2-\tilde{z}^2\right)^{1/2}$ to get

$$\begin{aligned}\left(A_0+\tilde{z}^2A_2\right)\left[-\frac{7}{2\tilde{r}}\left(\tilde{H}_0^2-\tilde{z}^2\right)+3\tilde{H}_0'\tilde{H}_0\right]+\left(A_0'+\tilde{z}^2A_2'\right)\left(\tilde{H}_0^2-\tilde{z}^2\right)\\ -3\left(\tilde{z}^2B_0+\tilde{z}^4B_2\right)+\left(\tilde{H}_0^2-\tilde{z}^2\right)\left(B_0+3\tilde{z}^2B_2\right)=0.\end{aligned} \tag{2.55}$$

We again separate this equation into by orders of $\tilde{z}$. This time, we obtain 3 separate equations. For $\tilde{z}^0$ we get

$$A_0\left(-\frac{7}{2\tilde{r}}\tilde{H}_0^2+3\tilde{H}_0'\tilde{H}_0\right)+\tilde{H}_0^2A_0'+B_0\tilde{H}_0^2=0. \tag{2.56}$$

For $\tilde{z}^2$ we write

$$-\frac{7}{2\tilde{r}}A_2\tilde{H}_0^2+\frac{7}{2\tilde{r}}A_0+3A_2\tilde{H}_0'\tilde{H}_0-A_0'+A_2'\tilde{H}_0^2-3B_0+3B_2\tilde{H}_0^2-B_0=0. \tag{2.57}$$

And finally, the equation for $\tilde{z}^4$ looks as follows

$$\frac{7}{2\tilde{r}}A_2-A_2'-6B_2=0, \tag{2.58}$$

which we will use to solve for B_2, but first let us calculate A_2'

$$A_2'=-\left(\Lambda\alpha\tilde{r}^{-5/2}\right)'=\frac{5}{2}\Lambda\alpha\tilde{r}^{-7/2}, \tag{2.59}$$

where the first equality stems from (2.46) and (2.38). Plugging this relation back into the equation (2.58), we calculate

$$B_2=\frac{7}{12}\frac{A_2}{\tilde{r}}-\frac{5}{12}\frac{\Lambda\alpha}{\tilde{r}^{7/2}}=-\frac{\Lambda\alpha}{\tilde{r}^{7/2}}. \tag{2.60}$$

From equation (2.56) it stems that

$$-A_0\left(\frac{7}{2\tilde{r}}-3\frac{\tilde{H}_0'}{\tilde{H}_0}\right)+A_0'+B_0=0. \tag{2.61}$$

We now add equations (2.61) and (2.56) in order to eliminate A_0'. These two equations determine $\tilde{H}_0$ and B_0. We are only interested in B_0, as we have already calculated $\tilde{H}_0$. After the addition we are left with

$$-\frac{7}{2\tilde{r}}A_2\tilde{H}_0^2+3A_2\tilde{H}_0'\tilde{H}_0+3A_0\frac{\tilde{H}_0'}{\tilde{H}_0}+A_2'\tilde{H}_0^2-3B_0+3B_2\tilde{H}_0^2=0. \tag{2.62}$$

Rearranging and plugging in known results we can write B_0 as follows

$$B_0=\frac{\alpha\tilde{H}_0^2}{\tilde{r}^{7/2}}\left[\Lambda+\frac{32}{15}\alpha^2\Lambda\frac{\mathrm{d}\ln\tilde{H}_0}{\mathrm{d}\ln\tilde{r}}-2\left(\frac{\mathrm{d}\ln\tilde{H}_0}{\mathrm{d}\ln\tilde{r}}\right)^2\right]. \tag{2.63}$$

This leads us to the vertical velocity $\tilde{v}_{z2}$ of the following form (Kluźniak and Kita [2000])

$$\tilde{v}_{z2}=\alpha\tilde{z}\frac{\tilde{H}_0^2}{\tilde{r}^{7/2}}\left[\Lambda\left(1-\frac{\tilde{z}^2}{\tilde{H}_0^2}\right)+\frac{32}{15}\alpha^2\Lambda\frac{\mathrm{d}\ln\tilde{H}_0}{\mathrm{d}\ln\tilde{r}}-2\left(\frac{\mathrm{d}\ln\tilde{H}_0}{\mathrm{d}\ln\tilde{r}}\right)^2\right]. \tag{2.64}$$

We have not yet used the vertical equation (2.32) and we will not do so now either. Solving this equation would lead to $\tilde{c}_{s2}$, which is a second order correction to the speed of sound, and we are not interested in that at the moment. Let us now recap what we have achieved in this section:

$$\tilde{\Omega}_2 = \frac{\tilde{H}_0^2}{\tilde{r}^{7/2}}\left[-\frac{3}{4}+\frac{1}{2}\frac{\mathrm{d}\ln\tilde{H}_0}{\mathrm{d}\ln\tilde{r}}+\frac{2}{15}\alpha^2\Lambda\left(1-6\frac{\tilde{z}^2}{\tilde{H}_0^2}\right)\right],$$

$$\tilde{v}_{r1} = \alpha\frac{\tilde{H}_0^2}{\tilde{r}^{5/2}}\left[\Lambda\left(1-\frac{\tilde{z}^2}{\tilde{H}_0^2}\right)+\frac{32}{15}\alpha^2\Lambda-2\frac{\mathrm{d}\ln\tilde{H}_0}{\mathrm{d}\ln\tilde{r}}\right],$$

$$\tilde{v}_{z2} = \alpha\tilde{z}\frac{\tilde{H}_0^2}{\tilde{r}^{7/2}}\left[\Lambda\left(1-\frac{\tilde{z}^2}{\tilde{H}_0^2}\right)+\frac{32}{15}\alpha^2\Lambda\frac{\mathrm{d}\ln\tilde{H}_0}{\mathrm{d}\ln\tilde{r}}-2\left(\frac{\mathrm{d}\ln\tilde{H}_0}{\mathrm{d}\ln\tilde{r}}\right)^2\right].$$

The vertical structure describes the formation of backflows nicely, see Figure 2.1 for reference. We plotted for three different values of the vertical coordinate $\tilde{z}=0$, $\tilde{z}=\tilde{H}_0$ and $\tilde{z}=\tilde{H}_0/\sqrt{6}$, which corresponds the height averaged value of the velocity. We averaged the radial velocity in the following manner

$$\langle\tilde{v}_{r1}\rangle = \frac{1}{\Sigma_0}\int_{-\tilde{H}_0}^{\tilde{H}_0}\tilde{\rho}_0\tilde{v}_{r1}d\tilde{z}, \tag{2.65}$$

where Σ_0 is the surface density given by

$$\Sigma_0 = \int_{-\tilde{H}_0}^{\tilde{H}_0}\tilde{\rho}_0 d\tilde{z}. \tag{2.66}$$

Calculating this yields

$$\langle\tilde{v}_{r1}\rangle = \tilde{v}_{r1}\left(\tilde{r},\tilde{z}=\frac{\tilde{H}_0}{\sqrt{6}}\right). \tag{2.67}$$

The vertically averaged value is very close to the value at the mid-plane. However, it cannot go into the positive values since it would mean that the matter is flowing outwards, which would not make sense as the matter would then have to be created somewhere. At the edge of the disk, the vertical velocity comes nowhere near the 0 mark, meaning there are absolutely no backflows at the edge. The relations between α, $\tilde{z}$ and $\tilde{r}_{\mathrm{stag}}$, which is the radius where the backflows start forming, can be further studied (see Kluźniak and Kita [2000]).

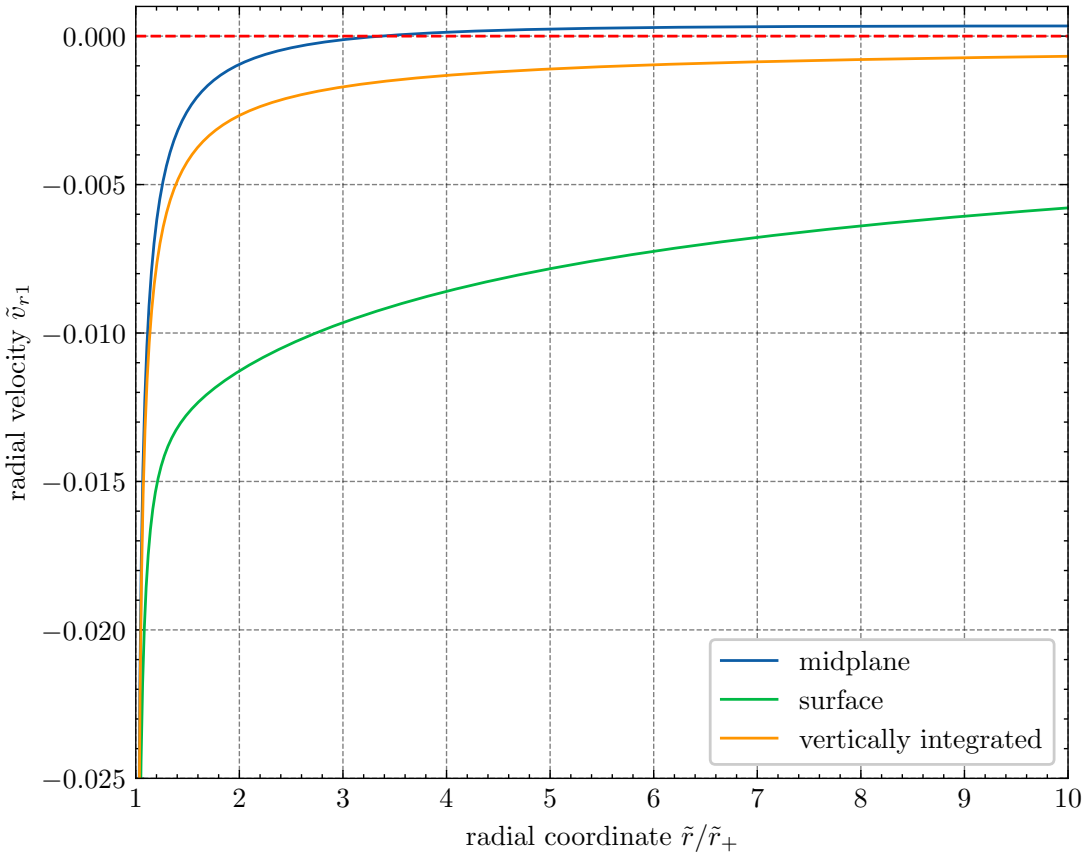

Figure 2.1: Plot showing the radial velocity in the outer disk at the midplane, surface and the vertically integrated value. We set $\alpha = 0.01$ and for the sake of simplicity we also set $\tilde{r}_+ = 1 = \dot{m}$. The divergent behaviour is clearly visible at the zero-torque radius. We see that the radial velocity diverges for all three different heights. In fact, a closer look at equation (2.52) reveals that the divergence is caused by height-independent terms. This gives us a reason to believe that in the boundary layer the quantities should be independent of z in the lowest order. The importance of proper vertical structure can also be seen in this plot since the vertically integrated radial velocity cannot describe the backflows near the midplane of the disk.

3. Boundary layer solutions

3.1 Perturbation theory

Perturbation theory is a powerful tool that helps us solve complex problems for which we are not able to find an exact solution. Perturbation theory offers an approximative solution whose functional dependence should be very similar to the actual solution. Even though we have not explicitly said so before, we had already used perturbation theory when we expanded all variables into a perturbation series of the following form: $y(x) = \sum_{i=0}^{N} \epsilon^i y_i(x)$, where y_i are the functions, we obtain by solving the given problem for each order of a small parameter ϵ. This is why we introduced the ϵ parameter the way we did and why our assumption of thin disk was important.

Perturbation problems can be divided into two subcategories – singular and regular (Bender and Orszag [1999]). Regular perturbation theory is suitable for problems, where already leading-order solution obtained by setting $\epsilon = 0$ provides a reasonable approximation. The higher order terms are just small corrections of the zeroth-order solution. An example of regular perturbation problem would be the equation $y'(x)+\epsilon y(x) = f(x)$ with a boundary condition $y(x_0) = A$, where x_0 and A are real numbers. In this case, the leading-order approximation is a solution of $y'_0(x) = f(x)$, which we obtained by setting $\epsilon = 0$. The boundary condition is then given by $y_0(x_0) = A$. The first order is determined by $y'_1(x) = -y_0(x)$ with $y_1(x_0) = 0$ as the boundary condition, and only serves as a correction. This is the approach KK use, and it is valid sufficiently far away from the inner edge of the disk.

On the other hand, a singular perturbation problem is described by equations that give either a trivial solution, or they cannot fulfil all the constraints imposed. A typical example of the sort is a differential equation, where the highest-order derivative term is multiplied by the expansion parameter. This is the approach that we will have to take in order to find global properties of the disk as our governing equations are singular. A simple example of this would be the differential equation $\epsilon y'(x) + y(x) = f(x)$ with the same boundary condition as in the case above. The nature of the equation changes when setting $\epsilon = 0$: originally first-order ODE is reduced to an algebraic equation. This change of nature can mean that the expansion is valid only for a certain range of x. The narrow region where the expansion is not valid is called a boundary layer, in which the term with the highest order of ϵ is not negligible anymore. Thus, we cannot expand and solve for each order separately in the boundary layer to get a reasonable approximation. This could be caused by the inability to meet the boundary conditions with the function obtained by the solution from the outer region. This is the case with the outer disk solution, which we just reviewed. Although, all the dimensionless equations (1.32)-(1.35) describing the accretion flow contain derivatives with respect to the radial coordinate, none of them appear in the zeroth-order equations (2.1)-(2.4), because they are always multiplied by higher-order quantities ($\sim \epsilon^2$ in the radial equation, or $\sim \epsilon$ in the rest). The radial dependence of the solution is therefore essentially described by algebraic equations, which do not provide enough freedom to satisfy the boundary condition at the interface between the

star and the disk. The silent assumption behind the regular perturbation method is that the solution described by an unknown function behaves "regularly", its derivatives are of the same order as the function itself. This is not the case in the boundary layer.

To get rid of this problem, we have to rescale both radial and vertical coordinates as well as the quantities in order to allow the solution to change fast in the radial direction. This essentially means that we zoom in the boundary layer. The proper scaling is acquired by requiring dominant balance when the term with the highest-order radial derivative appears in the leading-order equations. Dominant balance means that the most important terms for a given boundary condition are balanced i.e., they are of the same order of magnitude, and they are the most dominant. If we manage to obtain dominant balance, we can start to solve the rescaled equations. The new equations will yield a function f_i which is a solution valid in the boundary layer. Once we have the inner solution f_i and the outer solution f_o we will have to match them. Matching means that we require the limit of the inner solution as $X \to \infty$ to be equal to the limit of the outer solution as $x \to a$, where X is the variable of the inner region, x of the outer region and a is the point in whose neighbourhood is the boundary layer. We will construct the composite solution f on the entire region as follows $f = f_i + f_o -$ common limit. For further reference, see Bender and Orszag [1999].

3.2 Rescaled equations of motion

In this section, we use the knowledge of the outer solution and find a dominant balance so that we can achieve a non-singular solution in the neighbourhood of the zero-torque radius. We will denote all the scaled quantities with a hat and employ the following rescaling:

- $\tilde{r} = \tilde{r}_+ + \epsilon^\mu \hat{r}$
- $\tilde{v}_r = \epsilon^a \hat{v}_r$
- $\epsilon^2 \tilde{\Omega}_2 = \epsilon^c \hat{\omega}$
- $\tilde{z} = \epsilon^\nu \hat{z}$
- $\tilde{v}_z = \epsilon^b \hat{v}_z$
- $\tilde{c}_s = \epsilon^d \hat{c}_\mathrm{s}$

Notice how we did not scale the function $\tilde{\Omega}$, but only its second-order correction, as it is the first non-zero correction to the Keplerian angular frequency. We made this choice because the Keplerian angular frequency is a known function of $\tilde{r}$, and we know what the function looks like in the boundary layer. We thus defined a new function $\hat{\omega}$ which tells us how much the real value of angular frequency differs from the Keplerian value. Mathematically we can write $\hat{\omega} = \tilde{\Omega} - \tilde{\Omega}_\mathrm{K}$. See Figure 3.1 for reference. We first discuss how the scaling would look like in the outer region. Now that we know the solution, it is pretty simple. One might check for themselves that if we plug the following values $\mu = \nu = d = 0, a = 1, c = d = 2$ into the initial non-scaled equations from the Section 1.2, we obtain the scaled equations of motions as per discussed in Section 1.4. There are six unknown constants that we will have to find. Hence, we will need to find six equations to solve for μ, ν, a, b, c, d. Before we begin our calculations, we first need to discuss the orders of $\hat{\rho}, \hat{\eta}$ and $\hat{\xi}$ in terms of the six constants. From the equation for the polytropic speed of sound (1.4), we know that $c_\mathrm{s}^2 \sim P/\rho$. From the polytropic equation (1.2), it follows that $P \sim \rho^{(n+1)/n}$. This gives the following relation:

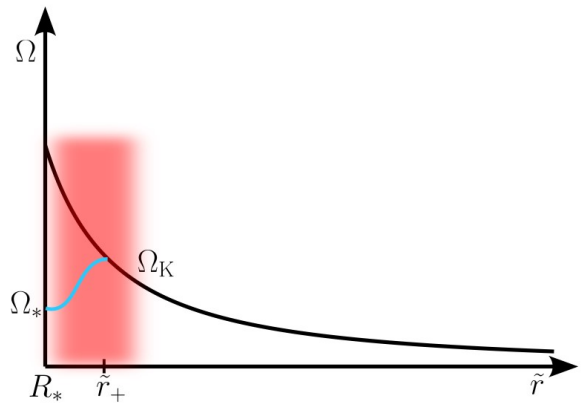

Figure 3.1: Schematic plot of the angular frequency. The blue line shows the expected angular frequency in the inner layer for a star rotating at a frequency Ω_*, which is below its Keplerian value at the stellar radius R_*. In the outer disk, the angular frequency is given by Ω_K up to second-order correction. In the further regions, the Keplerian frequency dominates and ω is negligible, however in the boundary layer in the neighbourhood of $\tilde{r}_+$, the correction ω becomes dominant. The red part represents the boundary layer.

$\rho \sim c_\mathrm{s}^{2n}$, which holds everywhere, hence we write $\tilde{\rho} = \epsilon^{2nd}\hat{\rho}$. From the definition of kinematic viscosity, we assumed we know that $\eta \sim c_\mathrm{s}^2\rho$, therefore we know that $\tilde{\eta} = \epsilon^{(2n+2)d}\hat{\eta}$. For $\hat{\xi}$ we assume that it is of the same order as $\hat{\eta}$. For the rescaled derivatives, we can write

$$\frac{\partial}{\partial\tilde{r}} = \frac{\partial}{\partial\hat{r}}\frac{\mathrm{d}\hat{r}}{\mathrm{d}\tilde{r}} = \epsilon^{-\mu}\frac{\partial}{\partial\hat{r}}. \tag{3.1}$$

Analogically for the $\tilde{z}$ derivative

$$\frac{\partial}{\partial\tilde{z}} = \frac{\partial}{\partial\hat{z}}\frac{\mathrm{d}\hat{z}}{\mathrm{d}\tilde{z}} = \epsilon^{-\nu}\frac{\partial}{\partial\hat{z}}. \tag{3.2}$$

This will be useful since we assume all the rescaled functions to be functions of their respective rescaled coordinates.

Let us now plug the rescaled variables into our equations from Section 1.4. For the continuity equation (1.35) we get:

$$\frac{\epsilon^{1+2nd-\mu+a}}{\tilde{r}_+ + \epsilon^\mu\hat{r}}\frac{\partial}{\partial\hat{r}}\left(\left(\tilde{r}_+ + \epsilon^\mu\hat{r}\right)\hat{\rho}\hat{v}_r\right) + \epsilon^{2nd-\nu+b}\frac{\partial}{\partial\hat{z}}\left(\hat{\rho}\hat{v}_z\right) = 0, \tag{3.3}$$

where we will ignore the terms $\epsilon^\mu\hat{r}$ since we assume that $\tilde{r}_+ \gg \epsilon^\mu\hat{r}$ and here we are interested in the leading-order solution only. Thus, we can either use Taylor expansion if it is in the denominator or it is of order μ lower than the term with $\tilde{r}_+$, which has to be greater than zero. If μ was equal to zero, there would be no scaling, and if it were less than zero, this would imply that $\hat{r} \gg \tilde{r}$ and we would be further than the outer region. We also know that $\tilde{r}_+$ is a constant, which simplifies the equation (3.3) to

$$\epsilon^{1+2nd-\mu+a}\frac{\partial}{\partial\hat{r}}\left(\hat{\rho}\hat{v}_r\right) + \epsilon^{2nd-\nu+b}\frac{\partial}{\partial\hat{z}}\left(\hat{\rho}\hat{v}_z\right) = 0. \tag{3.4}$$

Now, we want the terms in this equation to be of the same order to achieve dominant balance in this equation. Hence, we get our first equation for the constants

$$1 + a - \mu = b - \nu. \tag{3.5}$$

Interestingly enough, one can come to this conclusion just from geometry considerations. On the surface of the flow, we can write (Kluźniak and Kita [2000])

$$\frac{v_z}{v_r} = \frac{\frac{\mathrm{d}z}{\mathrm{d}t}}{\frac{\mathrm{d}r}{\mathrm{d}t}} = \pm\frac{\mathrm{d}H}{\mathrm{d}r}. \tag{3.6}$$

Comparing both sides of this equation and using our scalings, we get

$$b - a = 1 + \nu - \mu, \tag{3.7}$$

where we assumed that $\hat{H}$ is a characteristic value of $\hat{z}$ in the inner region. It is clear that equations (3.5) and (3.7) are equivalent.

Our next equation will be obtained from the vertical equation. As we have seen, the vertical momentum equation is in the outer disk dominated by the balance between the vertical gravity and the pressure gradient. In the following, we will assume that these terms are also present in the leading-order equations describing the flow in the vicinity of the zero-torque radius. Nevertheless, there may also appear other terms in the leading-order. Balancing these terms in the inner region, we have

$$\epsilon^{\nu}\frac{\hat{\tilde{z}}}{\tilde{r}_+^3} \sim \frac{3}{2}\epsilon^{2d-\nu}\frac{\partial\hat{c}_\mathrm{s}^2}{\partial\hat{\tilde{z}}}. \tag{3.8}$$

Comparing these terms, we end up with a simple equation

$$\nu = 2d - \nu. \tag{3.9}$$

In the outer disk, the radial equation is dominanted by the radial component of gravity and the centrifugal force. Consequently, the angular velocity is given by $\tilde{\Omega}_K$ at large distances. As discussed before, it is this assumption that leads to singular behaviour of the outer-disk solution. In order to obtain a regular solution, we have to include another term in the leading-order equation. The most natural choice is the radial pressure gradient that is increasingly important as $\tilde{r} \to \tilde{r}_+$. We therefore have in the inner region

$$-2\epsilon^c\hat{\omega}\tilde{\Omega}_0\tilde{r}_+ - \epsilon^{2c}\hat{\omega}^2\tilde{r}_+ = \frac{3}{2}\epsilon^{2+2\nu}\left(\frac{\hat{\tilde{z}}}{\tilde{r}_+^2}\right)^2 - \frac{3}{2}\epsilon^{2+2d-\mu}\frac{\partial\hat{c}_\mathrm{s}^2}{\partial\hat{r}}. \tag{3.10}$$

We can ignore the term involving $\hat{\omega}^2$ because it is of a lower order than the term involving $\hat{\omega}$. Hence, we are left with three terms: the term involving $\hat{\omega}$, the gravitational term and the pressure term. It seems reasonable to us to balance the pressure term with the first term on the left-hand side because we want to express that $\hat{\omega}$ becomes more important in the inner region and the gravity term is just a correction, which gets smaller as the disk gets thinner. We thus balance the said terms yielding another constraint

$$c = 2 + 2d - \mu. \tag{3.11}$$

Three done, three to go. Let us now examine a constant of integration from equation (2.22). Rescaling the equation, one gets

$$\epsilon\dot{m} = -\epsilon^{2nd+a+\nu}\tilde{r}_+ \int_{-\infty}^{\infty} \hat{\rho}\hat{v}_r d\hat{z}. \tag{3.12}$$

Balancing both sides of this equation yields our fourth constraint

$$1 = 2nd + a + \nu, \tag{3.13}$$

where we chose to work with general polytropic index n.

For the last two equations we will have to study the azimuthal equation. Rescaled version takes the following form

$$\begin{aligned}\epsilon^{1+2nd+a}\frac{\hat{\rho}\hat{v}_r}{\tilde{r}_+^2}\left[\frac{\mathrm{d}(\tilde{r}_+^2\tilde{\Omega}_0)}{\mathrm{d}\tilde{r}} + \epsilon^{c-\mu}\frac{\partial(\tilde{r}_+^2\hat{\omega})}{\partial\hat{r}}\right] + \epsilon^{2nd+b+c-\nu}\hat{\rho}\hat{v}_z\frac{\partial\hat{\omega}}{\partial\hat{z}} = \\ \epsilon^{2+(2n+2)d-\mu}\frac{1}{\tilde{r}_+^3}\left[\frac{\partial}{\partial\hat{r}}\left(\hat{\eta}\tilde{r}_+^3\frac{\mathrm{d}\tilde{\Omega}_0}{\mathrm{d}\tilde{r}}\right)\right] \\ +\epsilon^{2+(2n+2)d-2\mu+c}\frac{1}{\tilde{r}_+^3}\left[\frac{\partial}{\partial\hat{r}}\left(\hat{\eta}\tilde{r}_+^3\frac{\partial\hat{\omega}}{\partial\hat{r}}\right)\right] + \epsilon^{(2n+2)d-2\nu+c}\frac{\partial}{\partial\hat{z}}\left(\hat{\eta}\frac{\partial\hat{\omega}}{\partial\hat{z}}\right),\end{aligned} \tag{3.14}$$

where we chose to write the terms involving $\tilde{\Omega}_0$ as derivatives with respect to $\tilde{r}$ since we know how this function behaves and scaling makes it a constant in the inner layer. We want to balance the terms in the first square bracket, since the second term becomes more dominant in the boundary layer, as one can conclude from the second constant of integration. We thus get a fifth constrain, which is that

$$0 = c - \mu. \tag{3.15}$$

The last constraint will be obtained by balancing the entire first bracket on the left-hand side with the first two terms on the right-hand side. As was demonstrated before, the divergent terms depend only weakly on the vertical coordinate close to $\tilde{r}_+$. Our choice compares all the terms with radial derivatives, which should be more important in the boundary layer. The last equation therefore is

$$1 + 2nd + a = 2 + (2n+2)d - \mu. \tag{3.16}$$

Let us briefly recap the equations before we solve them:

- $1 + a - \mu = b - \nu$,
- $1 = 2nd + a + \nu$,
- $\nu = d$,
- $c = \mu$,
- $c = 2 + 2d - \mu$,
- $1 + 2nd + a = 2 + (2n+2)d - \mu$.

Solving this system of equations yields

$$a = b = d = \nu = \frac{1}{2n+2}, \tag{3.17}$$

$$c = \mu = 1 + \frac{1}{2n+2} = 1 + a. \tag{3.18}$$

Let us now plug in these constants back into our equations. For the leading order we can write

$$\begin{aligned}\hat{v}_r\frac{\partial\hat{v}_r}{\partial\hat{r}}+\hat{v}_z\frac{\partial\hat{v}_r}{\partial\hat{z}}-2\tilde{\Omega}_0\hat{\omega}\tilde{r}_+ &= -\frac{3}{2}\frac{\partial\hat{c}_\mathrm{s}^2}{\partial\hat{r}}\\ +\frac{2}{\hat{\rho}}\frac{\partial}{\partial\hat{r}}\left(\hat{\eta}\frac{\partial\hat{v}_r}{\partial\hat{r}}\right)+\frac{1}{\hat{\rho}}\frac{\partial}{\partial\hat{z}}\left(\hat{\eta}\frac{\partial\hat{v}_r}{\partial\hat{z}}\right)+\frac{1}{\hat{\rho}}\frac{\partial}{\partial\hat{z}}\left(\hat{\eta}\frac{\partial\hat{v}_z}{\partial\hat{r}}\right)&\\ +\frac{1}{\hat{\rho}}\frac{\partial}{\partial\hat{r}}\left[\left(\hat{\xi}-\frac{2}{3}\hat{\eta}\right)\left(\frac{\partial\hat{v}_r}{\partial\hat{r}}\right)\right]+\frac{1}{\hat{\rho}}\frac{\partial}{\partial\hat{r}}\left[\left(\hat{\xi}-\frac{2}{3}\hat{\eta}\right)\frac{\partial\hat{v}_z}{\partial\hat{z}}\right],&\end{aligned}\tag{3.19}$$

$$\hat{\rho}\hat{v}_r\left(\frac{\mathrm{d}\tilde{\Omega}_0}{\mathrm{d}\tilde{r}}+\frac{\partial\hat{\omega}}{\partial\hat{r}}\right)+\hat{\rho}\hat{v}_z\frac{\partial\hat{\omega}}{\partial\hat{z}}=\frac{\partial}{\partial\hat{r}}\left(\hat{\eta}\frac{\mathrm{d}\tilde{\Omega}_0}{\mathrm{d}\tilde{r}}\right)+\frac{\partial}{\partial\hat{r}}\left(\hat{\eta}\frac{\partial\hat{\omega}}{\partial\hat{r}}\right)+\frac{\partial}{\partial\hat{z}}\left(\hat{\eta}\frac{\partial\hat{\omega}}{\partial\hat{z}}\right),\tag{3.20}$$

$$\begin{aligned}\hat{v}_r\frac{\partial\hat{v}_z}{\partial\hat{r}}+\hat{v}_z\frac{\partial\hat{v}_z}{\partial\hat{z}} &= -\frac{\hat{z}}{\tilde{r}_+^3}-\frac{3}{2}\frac{\partial\hat{c}_\mathrm{s}^2}{\partial\hat{z}}+\frac{2}{\hat{\rho}}\frac{\partial}{\partial\hat{z}}\left(\hat{\eta}\frac{\partial\hat{v}_z}{\partial\hat{z}}\right)+\frac{1}{\hat{\rho}}\frac{\partial}{\partial\hat{r}}\left(\hat{\eta}\frac{\partial\hat{v}_z}{\partial\hat{r}}\right)+\\ &\frac{1}{\hat{\rho}}\frac{\partial}{\partial\hat{r}}\left(\hat{\eta}\frac{\partial\hat{v}_r}{\partial\hat{z}}\right)+\frac{1}{\hat{\rho}}\frac{\partial}{\partial\hat{z}}\left[\left(\hat{\xi}-\frac{2}{3}\hat{\eta}\right)\frac{\partial\hat{v}_z}{\partial\hat{z}}\right]\\ &+\frac{1}{\hat{\rho}}\frac{\partial}{\partial\hat{z}}\left[\left(\hat{\xi}-\frac{2}{3}\hat{\eta}\right)\frac{\partial\hat{v}_r}{\partial\hat{r}}\right],\end{aligned}\tag{3.21}$$

$$\frac{\partial}{\partial\hat{r}}\left(\hat{\rho}\hat{v}_r\right)+\frac{\partial}{\partial\hat{z}}\left(\hat{\rho}\hat{v}_z\right)=0.\tag{3.22}$$

We used the fact that $\tilde{r}_+$ is a constant; hence, we could get rid of terms which had the pre-factor $1/\tilde{r}^k$ and $\tilde{r}^k$ inside a derivative in the $\tilde{r}$ direction. In the same manner as in Section 2.4 we shall write out some important relations:

$$\frac{\hat{\eta}}{\hat{\rho}}=\frac{2}{5}\alpha\frac{\hat{c}_\mathrm{s}^2}{\tilde{\Omega}_0},$$

$$\frac{1}{\hat{\rho}}\frac{\partial\hat{\eta}}{\partial\hat{r}}=\frac{\alpha}{\tilde{\Omega}_0}\frac{\partial\hat{c}_\mathrm{s}^2}{\partial\hat{r}},$$

$$\frac{1}{\hat{\rho}}\frac{\partial\hat{\eta}}{\partial\hat{z}}=\frac{\alpha}{\tilde{\Omega}_0}\frac{\partial\hat{c}_\mathrm{s}^2}{\partial\hat{z}}.$$

The equations (3.19)-(3.22) are non-linear partial differential equations in $\hat{r}$ and $\hat{z}$. Motivated by KK outer disk second-order solution, we attempt to solve these equations in a similar fashion. Namely, we will employ the following ansatz $\hat{v}_r=A(\hat{r})$, $\hat{c}_\mathrm{s}^2=C(\hat{r})+\hat{z}^2D(\hat{r})$, $\hat{v}_z=\hat{z}E(\hat{r})$, $\hat{\omega}=W(\hat{r})$, where A, C, D, E and W are functions to be determined from the equations by comparing the terms with the same order of $\tilde{z}$. This ansatz takes into account the behaviour of the outer disk solution as $\tilde{r}\to\tilde{r}_+$. We know that the quantities $\tilde{v}_r$, $\tilde{v}_z/z$ and $\tilde{\Omega}_2$ depend on the vertical coordinate weakly in the neighbourhood of $\tilde{r}_+$ since all the divergent terms are height-independent. The terms that do depend on $\tilde{z}$ serve as small corrections as was demonstrated on Figure 2.1 for the radial velocity. After plugging in the ansatz into our rescaled equations, we arrive at equations with polynomial dependence on the vertical coordinate. Comparing terms of the

same power of $\hat{z}$, we obtain a system of ODEs governing the functions A, C, D, E and W.

However, the system is overdetermined. We obtain more constraints than the number of variables we are solving for. The continuity, azimuthal and radial equations contain terms proportional to $\hat{z}^2$ as well as height-independent terms. The vertical equation yields terms proportional to $\hat{z}$ and $\hat{z}^3$. This is in total 8 constraints for just 5 variables. Such systems of equations usually have only trivial solutions, unless all the constraints are compatible with each other.

In our case, the system is consistent when three of the equations are dependent on the rest. Unfortunatelly, as the system is highly non-linear, we were not able to demonstrate its inconsistency, nor have we been able to prove that the system is overdetermined. Nevertheless, we would like to note that the system still likely leads to only a trivial solution if one introduces a more complicated vertical structure than the one introduced by our ansatz.

Finally, during our attempt at solving this system, we have found that the radial and vertical Euler equations simplify significantly if we rescale the α parameter. This makes further analysis easier as we can work with less complicated systems of equations. This finding server us as motivation for the next chapter, where we explore in more details flows with a small values of the viscosity parameter. For this type of flows, we will first demonstrate the inconsistency of our ansatz. Next, we will suggest how to correct the ansatz to obtain a self-consistent system of equations.

3.3 Low-viscosity accretion flows

In this section, we restrict ourselves to flow with a low value of the viscosity parameter α. As mentioned in the introduction, α has to be less than one in order for the turbulence to be subsonic. We consider flows where the α parameter is scaled by some power of the thickness parameter ϵ. Therefore, we rescale the α parameter as $\alpha = \epsilon^q \hat{\alpha}$, where $\hat{\alpha}$ is of order unity and $q > 0$. We were motivated to do this by the fact, that for subsonic turbulence, it has to hold that $\alpha < 1$. It also seems reasonable to use this scaling as it gets rid of the problematic term in the lowest order. The additional scaling gives us another unknown q. We will leave q to be a free parameter. With this new scaling we obtain the following equations:

- $1 + a - \mu = b - \nu$,
- $1 + q = 2nd + a + \nu$,
- $\nu = d$,
- $c = \mu$,
- $c = 2 + 2d - \mu$,
- $1 + 2nd + a = 2 + (2n+2)d - \mu + q$.

We needed to look back at equation (3.12) and realise that $\dot{m}$ is no longer $O(1)$, but $O(\epsilon^q)$, since $\tilde{v}_{r1}$ depends linearly on α which is being scaled. Solving this system yields

$$\nu = d = \frac{1}{2n+2}, \tag{3.23}$$

$$c = \mu = d + 1, \tag{3.24}$$

$$a = b = d + q. \tag{3.25}$$

As stated before, q is a free parameter; however, we do have one constraint. We need the velocities to be subsonic, which leads us to the following observation:

$$\tilde{v}_r^2 \leq \tilde{c}_\mathrm{s}^2 \Leftrightarrow \epsilon^a \hat{v}_r \leq \epsilon^d \hat{c}_\mathrm{s}, \tag{3.26}$$

which is satisfied for $q \geq 0$. Similarly for the vertical velocity. This knowledge greatly simplifies the equations since we know that any term with ϵ^q is of a lower order for any q greater than zero. We have already discussed the case of $q = 0$ as it was the scaling we used at first. With the assumption of $q > 0$ we can write the equations in the lowest order as:

$$2\tilde{\Omega}_0 \hat{\omega} \tilde{r}_+ = \frac{3}{2} \frac{\partial \hat{c}_\mathrm{s}^2}{\partial \hat{r}}, \tag{3.27}$$

$$\hat{\rho}\hat{v}_r \left(\frac{\mathrm{d}\tilde{\Omega}_0}{\mathrm{d}\tilde{r}} + \frac{\partial \hat{\omega}}{\partial \hat{r}} \right) + \hat{\rho}\hat{v}_z \frac{\partial \hat{\omega}}{\partial \hat{z}} = \frac{\partial}{\partial \hat{r}} \left(\hat{\eta} \frac{\mathrm{d}\tilde{\Omega}_0}{\mathrm{d}\tilde{r}} \right) + \frac{\partial}{\partial \hat{r}} \left(\hat{\eta} \frac{\partial \hat{\omega}}{\partial \hat{r}} \right) + \frac{\partial}{\partial \hat{z}} \left(\hat{\eta} \frac{\partial \hat{\omega}}{\partial \hat{z}} \right), \tag{3.28}$$

$$0 = -\frac{\hat{z}}{\tilde{r}_+^3} - \frac{3}{2} \frac{\partial \hat{c}_\mathrm{s}^2}{\partial \hat{z}}, \tag{3.29}$$

$$\frac{\partial}{\partial \hat{r}} \left(\hat{\rho}\hat{v}_r \right) + \frac{\partial}{\partial \hat{z}} \left(\hat{\rho}\hat{v}_z \right) = 0. \tag{3.30}$$

As we can see, the continuity and azimuthal equations are still the same, but the vertical and radial equations change significantly. The rest of the terms in equations (3.19) and (3.21) are of order q higher than the lowest terms.

3.4 Various assumptions about the vertical profile of the disk

In this section, we first demonstrate that our assumptions about the vertical structure introduced at the end of Section 3.2 do not lead to a self-consistent solution in the case of low-viscosity accretion flows. Next, we demonstrate that we can fix this situation by introducing a non-trivial vertical structure of the velocity field.

3.4.1 Trivial profile of the velocity field

In this subsection, we will employ the ansatz introduced in Section 3.2: $\hat{v}_r = A(\hat{r})$, $\hat{c}_\mathrm{s}^2 = C(\hat{r}) + \hat{z}^2 D(\hat{r})$, $\hat{v}_z = \hat{z} E(\hat{r})$, $\hat{\omega} = W(\hat{r})$. We will again separate by orders of $\hat{z}$. In this case, we obtain 7 constraints for 5 unknowns. In comparison with the case discussed in Section 3.2, the vertical equation (3.29) gives just terms that depend linearly on $\hat{z}$ and one height-independent term.

The radial equation in $\hat{z}^2$ yields

$$0 = D', \tag{3.31}$$

hence D is a constant in $\hat{r}$. For $\hat{z}^0$ we can write

$$C' = \frac{4}{3} \tilde{\Omega}_0 W \tilde{r}_+. \tag{3.32}$$

Similarly for the vertical equation we write

$$D = -\frac{1}{3\tilde{r}_+^3}, \tag{3.33}$$

which is consistent with equation (3.31). Let us now divide the azimuthal equation (3.28) by the density $\hat{\rho}$ and simplify as

$$\hat{v}_r \left(\frac{\mathrm{d}\tilde{\Omega}_0}{\mathrm{d}\tilde{r}} + \frac{\partial \hat{\omega}}{\partial \hat{r}} \right) = \frac{1}{\hat{\rho}} \frac{\partial}{\partial \hat{r}} \left(\hat{\eta} \frac{\mathrm{d}\tilde{\Omega}_0}{\mathrm{d}\tilde{r}} \right) + \frac{1}{\hat{\rho}} \frac{\partial}{\partial \hat{r}} \left(\hat{\eta} \frac{\partial \hat{\omega}}{\partial \hat{r}} \right). \tag{3.34}$$

Differentiating and employing the list of equalities we can write

$$A \left(\tilde{\Omega}_0' + W' \right) = \frac{2}{5} \frac{\hat{\alpha}}{\tilde{\Omega}_0} \left(C + \hat{z}^2 D \right) W'' + \frac{\hat{\alpha}}{\tilde{\Omega}_0} \left(\tilde{\Omega}_0' + W' \right) C', \tag{3.35}$$

where we used our ansatz and also the fact that $D' = 0$. Note that the sign "′" means the respective derivative - for terms with a tilde, it is a derivative with respect to $\tilde{r}$, and for the rest of the terms, it means the derivative with respect to $\hat{r}$. Terms with $\hat{z}^2$ give

$$W'' = 0 \Rightarrow W = \kappa \hat{r} + \beta, \tag{3.36}$$

where κ and β are yet unknown constants. For $\hat{z}^0$ we can write

$$A \left(\tilde{\Omega}_0' + W' \right) = \frac{\hat{\alpha}}{\tilde{\Omega}_0} \left(\tilde{\Omega}_0' + W' \right) C'. \tag{3.37}$$

Before we get to the continuity equation, we remind ourselves that for $n = 3/2$ we have $\hat{\rho} = \hat{c}_s^3 = (C + \hat{z}^2 D)^{3/2}$. We can now write

$$A' \left(C + \hat{z}^2 D \right) + \frac{3}{2} A C' + E \left(C + \hat{z}^2 D \right) + 3 \hat{z}^2 E D = 0, \tag{3.38}$$

where the height-independent part is

$$A' C + \frac{3}{2} A C' + E C = 0, \tag{3.39}$$

which gives a relation between A, E and C. We already know what W is, so we can then use the relation (3.32) to calculate for C and then the relation (3.37) to obtain a result for A. Hence, we could now calculate E. We have yet to examine the last equation stemming from the continuity equation for the terms with $\hat{z}^2$. We can write this equation as

$$A' = -4E, \tag{3.40}$$

which unfortunately leads to all constants being zero. Therefore, all the quantities vanish and we arrive at a trivial solution. This demonstrates that our original ansatz does not provide a non-trivial solution in the case of low-viscosity flow.

3.4.2 Parabolic profile of the radial velocity

The previous result shows that our ansatz is too simple, and that we need to consider a non-trivial vertical structure of the velocity field. The origin of the inconsistency of the previous assumptions can be traced to W being linear in $\hat{r}$, which causes the radial dependence of the rest of the terms to be of polynomial nature. We can obtain a more general dependence on $\hat{r}$ for W if the left-hand size of the azimuthal equation (3.35) has some vertical structure. Therefore, we will now try to add vertical structure for the radial velocity $\hat{v}_r$. In this subsection, we will thus assume $\hat{v}_r = A(\hat{r}) + \hat{z}^2 B(\hat{r})$, $\hat{c}_\mathrm{s}^2 = C(\hat{r}) + \hat{z}^2 D(\hat{r})$, $\hat{v}_z = \hat{z}E(\hat{r})$, $\hat{\omega} = W(\hat{r})$. As one can see, this does not change the results from the radial and vertical equations (3.31)-(3.33). We only need to correct the azimuthal and continuity equations. The azimuthal equation now becomes

$$\left(A + \hat{z}^2 B\right)\left(\tilde{\Omega}_0' + W'\right) = \frac{2}{5}\frac{\hat{\alpha}}{\tilde{\Omega}_0}\left(C + \hat{z}^2 D\right)W'' + \frac{\hat{\alpha}}{\tilde{\Omega}_0}\left(\tilde{\Omega}_0' + W'\right)C', \tag{3.41}$$

which seemingly changes only the equation for $\hat{z}^2$-component, but since W'' is no longer zero, both components are affected by this change. The continuity equation becomes

$$\left(A' + \hat{z}^2 B'\right)\left(C + \hat{z}^2 D\right) + \frac{3}{2}\left(A + \hat{z}^2 B\right)C' + E\left(C + \hat{z}^2 D\right) + 3\hat{z}^2 ED = 0, \tag{3.42}$$

which changes in the order of $\hat{z}^2$ and also yields a new relation in $\hat{z}^4$. The new equation implies that B is a constant in $\hat{r}$, which helps us solve the azimuthal equation in the order of $\hat{z}^2$. The said equation is of the following form

$$B\left(\tilde{\Omega}_0' + W'\right) = \frac{2}{5}\frac{\hat{\alpha}}{\tilde{\Omega}_0}DW'', \tag{3.43}$$

which we can use to solve for W. The solution is a linear combination of a linear term in $\hat{r}$, an exponential term in $\hat{r}$ and a constant. We can try to solve the rest of the equation, but we will again be left with one more equation than is the number of variables. The last equation may be used to calculate the constants, which yet again leads to all quantities being zero. Therefore, this attempt does not lead to a non-trivial solution either.

3.4.3 Cubic profile of the vertical velocity

We traced the fact that the second ansatz does not provide a non-trivial solution to be caused by B being a constant. We now try to fix this issue by allowing a more general dependence of the vertical velocity on height. We assume: $\hat{v}_r = A(\hat{r}) + \hat{z}^2 B(\hat{r})$, $\hat{c}_\mathrm{s}^2 = C(\hat{r}) + \hat{z}^2 D(\hat{r})$, $\hat{v}_z = \hat{z}E(\hat{r}) + \hat{z}^3 F$, $\hat{\omega} = W(\hat{r})$. Let us recap the equations with this latest ansatz so that one does not get lost in the amount of equations presented:

$$0 = -\frac{\hat{z}}{\tilde{r}_+^3} - \frac{3}{2}\frac{\partial \hat{c}_\mathrm{s}^2}{\partial \hat{z}},$$

$$2\tilde{\Omega}_0 W \tilde{r}_+ = \frac{3}{2}\frac{\partial \hat{c}_\mathrm{s}^2}{\partial \hat{r}},$$

$$\left(A' + \hat{z}^2 B'\right)\left(C + \hat{z}^2 D\right) + \frac{3}{2}\left(A + \hat{z}^2 B\right) C' + \left(E + 3\hat{z}^2 F\right)\left(C + \hat{z}^2 D\right) + 3\hat{z}^2\left(E + \hat{z}^2 F\right) D = 0,$$

$$\left(A + \hat{z}^2 B\right)\left(\tilde{\Omega}_0' + W'\right) = \frac{2}{5}\frac{\hat{\alpha}}{\tilde{\Omega}_0}\left(C + \hat{z}^2 D\right) W'' + \frac{\hat{\alpha}}{\tilde{\Omega}_0}\left(\tilde{\Omega}_0' + W'\right) C'.$$

We chose to write the vertical and radial equations in their unseparated form because of the following reason. The vertical equation is actually identical to the vertical equation in the inner region, so we know the solution for $\hat{c}_s^2$. We chose to leave the ansatz form in the equations before, as it might be easier to work with C and D and just at the end of our calculations plug in for them. We write the speed of sound in the inner region as

$$\hat{c}_{\mathrm{s}}^2 = \frac{\tilde{\Omega}_0^2}{3}\left(\hat{H}^2 - \hat{z}^2\right). \tag{3.44}$$

From this we can determine that

$$C = \frac{\tilde{\Omega}_0^2}{3}\hat{H}^2, \quad D = -\frac{\tilde{\Omega}_0^2}{3}. \tag{3.45}$$

The result for D was already known from equation (3.33). However, we did not know what C should be. This is also the point we remind ourselves that $\tilde{\Omega}_0$ is a constant in the inner layer. The radial equation gives a relation between the disk semi-thickness $\hat{H}$ and the angular velocity $\hat{\omega}$. If we manage to find the radial dependence of the disk semi-thickness, we will then be able to solve for W. This will lead us to the vertical velocity given by A and B from the azimuthal equation. We will then be able to calculate E and F yielding the vertical velocity. However, we will have one redundant equation yet again since we will try to solve for $\hat{H}$ from the same equation we used while deriving the disk thickness in Section 2.3. The redundant equation may serve as a consistency check. We will now express all the quantities as functions of $\hat{H}$. Beginning with W, the vertical equation yields

$$W = \frac{\tilde{\Omega}_0}{4\tilde{r}_+}\frac{\mathrm{d}\hat{H}^2}{\mathrm{d}\hat{r}}. \tag{3.46}$$

We are now able to express A as well as B from the azimuthal equation as follows

$$B = -\frac{\hat{\alpha}\tilde{\Omega}_0 \frac{\mathrm{d}^3\hat{H}^2}{\mathrm{d}\hat{r}^3}}{30\left(-\frac{3}{2} + \frac{1}{4}\frac{\mathrm{d}^2\hat{H}^2}{\mathrm{d}\hat{r}^2}\right)}, \tag{3.47}$$

and

$$A = \frac{\hat{\alpha}\tilde{\Omega}_0\hat{H}^2\frac{\mathrm{d}^3\hat{H}^2}{\mathrm{d}\hat{r}^3}}{30\left(-\frac{3}{2} + \frac{1}{4}\frac{\mathrm{d}^2\hat{H}^2}{\mathrm{d}\hat{r}^2}\right)} + \frac{\hat{\alpha}\tilde{\Omega}_0}{3}\frac{\mathrm{d}\hat{H}^2}{\mathrm{d}\hat{r}}. \tag{3.48}$$

We thus are able write the radial velocity $\hat{v}_r$ in the following form

$$\hat{v}_r = \hat{\alpha}\tilde{\Omega}_0\hat{H}^2\left[\frac{\frac{\mathrm{d}^3\hat{H}^2}{\mathrm{d}\hat{r}^3}}{30\left(-\frac{3}{2} + \frac{1}{4}\frac{\mathrm{d}^2\hat{H}^2}{\mathrm{d}\hat{r}^2}\right)}\left(1 - \frac{\hat{z}^2}{\hat{H}^2}\right) + \frac{1}{3}\frac{\mathrm{d}\ln\hat{H}^2}{\mathrm{d}\hat{r}}\right]. \tag{3.49}$$

We could also express the vertical velocity in terms of $\hat{H}$ and its derivatives. However, we will just express it in terms of A and B as we are not currently interested in the vertical velocity. From the continuity equation in $\hat{z}^4$, we can get

$$F = -\frac{B'}{6}. \tag{3.50}$$

From $\hat{z}^0$ in continuity equation, it stems that

$$E = -A' - \frac{3}{2}\frac{C'}{C}A, \tag{3.51}$$

which after plugging in for C and some adjustments can be written as

$$E = -\frac{1}{\hat{H}^3}\frac{\mathrm{d}}{\mathrm{d}\hat{r}}\left(A\hat{H}^3\right). \tag{3.52}$$

Now that we have expressed all the variables in terms of $\hat{H}$ and its derivatives, all we have to do is actually calculate $\hat{H}$. We will try to find an expression for $\hat{H}$ the same way as in the outer solution; hence we take a look at equation (2.27), which changes in the inner layer. We can write the difference of angular momenta in the neighbourhood of $\tilde{r}_+$ as follows:

$$\tilde{\tilde{j}}_K - \tilde{\tilde{j}}_+ = \sqrt{\tilde{r}_+ + \epsilon^c\hat{r}} - \sqrt{\tilde{r}_+} \doteq \sqrt{\tilde{r}_+} + \frac{\epsilon^c\hat{r}}{2\sqrt{\tilde{r}_+}} - \sqrt{\tilde{r}_+}. \tag{3.53}$$

Thus, we can rewrite equation (2.27) as

$$\dot{m}\left(\frac{\hat{r}}{2\sqrt{\tilde{r}_+}} + W\tilde{r}_+^2\right) = -\tilde{r}_+^3\left(\tilde{\Omega}_0' + W'\right)\int_{-\hat{H}}^{\hat{H}}\hat{\eta}\mathrm{d}\hat{Z}, \tag{3.54}$$

which stems from us balancing the terms on the left-hand side with the right-hand side in our scaling. We can plug in for W from equation (3.46) giving us

$$\dot{m}\left(\frac{\hat{r}}{2\sqrt{\tilde{r}_+}} + \frac{\tilde{r}_+\tilde{\Omega}_0}{4}\frac{\mathrm{d}\hat{H}^2}{\mathrm{d}\hat{r}}\right) = -\tilde{r}_+^3\left(-\frac{3\tilde{\Omega}_0}{2\tilde{r}_+} + \frac{\tilde{\Omega}_0}{4\tilde{r}_+}\frac{\mathrm{d}^2\hat{H}^2}{\mathrm{d}\hat{r}^2}\right)\int_{-\hat{H}}^{\hat{H}}\hat{\eta}\mathrm{d}\hat{Z}. \tag{3.55}$$

We now have to integrate $\hat{\eta}$, which we can write as

$$\hat{\eta} = \frac{2\hat{\alpha}}{3\tilde{\Omega}_0}\left(\frac{\tilde{\Omega}_0^2}{5}\left(\hat{H}^2 - \hat{Z}^2\right)\right)^{5/2}. \tag{3.56}$$

The integration is given by equation (2.28). We finally obtain

$$\dot{m}\left(\frac{\hat{r}}{2\sqrt{\tilde{r}_+}} + \frac{\tilde{r}_+\tilde{\Omega}_0}{4}\frac{\mathrm{d}\hat{H}^2}{\mathrm{d}\hat{r}}\right) = \tilde{r}_+^2\hat{\alpha}\frac{\tilde{\Omega}_0^5\pi\hat{H}^6}{16\cdot 5^{3/2}} - \tilde{r}_+^2\hat{\alpha}\frac{\tilde{\Omega}_0^5\pi\hat{H}^6}{16\cdot 6\cdot 5^{3/2}}\frac{\mathrm{d}^2\hat{H}^2}{\mathrm{d}\hat{r}^2}. \tag{3.57}$$

In order to simplify notation we introduce a new variable: $y(\hat{r}) = \hat{H}^2(\hat{r})$. With this, we have obtained a second-order non-linear differential equation of the following form

$$\tau\hat{r} + \beta y'(\hat{r}) = \gamma y^3(\hat{r}) - \lambda y^3(\hat{r})y''(\hat{r}), \tag{3.58}$$

τ, β, γ and λ are constants equal to

$$\tau = \frac{\dot{m}}{2\sqrt{\tilde{r}_+}}, \tag{3.59}$$

$$\beta = \frac{\dot{m}\tilde{r}_+\tilde{\Omega}_0}{4}, \tag{3.60}$$

$$\gamma = \tilde{r}_+^2\hat{\alpha}\frac{\tilde{\Omega}_0^5\pi}{16\cdot 5^{3/2}}, \tag{3.61}$$

$$\lambda = \tilde{r}_+^2\hat{\alpha}\frac{\tilde{\Omega}_0^5\pi}{16\cdot 6\cdot 5^{3/2}}. \tag{3.62}$$

Let us now divide equation (3.58) by λ and introduce new constants $\hat{\tau} = \tau/\lambda$, $\hat{\beta} = \beta/\lambda$ and $\hat{\gamma} = \gamma/\lambda$. We will also rescale this equation by rescaling y and $\hat{r}$ as

$$y = y_0\tilde{y}, \quad \hat{r} = R_0\tilde{R}, \tag{3.63}$$

where y_0 and R_0 are constants and $\tilde{y}$ and $\tilde{R}$ are the new variables. We will now rewrite equation (3.58) in terms of these new variables. We can write

$$\hat{\tau}R_0\tilde{R} + \hat{\beta}\frac{y_0}{R_0}\tilde{y}'(\tilde{R}) = \hat{\gamma}y_0^3\tilde{y}^3(\tilde{R}) - \frac{y_0^4}{R_0^2}\tilde{y}^3(\tilde{R})\tilde{y}''(\tilde{R}). \tag{3.64}$$

Let us now divide this equation by y_0^4/R_0^2 and then set the constants in front of the second term on the left-hand side and the first term on the right equal to 1. We have some freedom here as y_0 and R_0 are yet undetermined. The equation now becomes

$$\hat{\tau}\frac{R_0^3}{y_0^4}\tilde{R} + \tilde{y}'(\tilde{R}) = \tilde{y}^3(\tilde{R}) - \tilde{y}^3(\tilde{R})\tilde{y}''(\tilde{R}). \tag{3.65}$$

By setting the terms equal to one we get two equations for the constants. The equations read

$$\hat{\beta}\frac{R_0}{y_0^3} = 1, \tag{3.66}$$

and

$$\hat{\gamma}\frac{R_0^2}{y_0} = 1. \tag{3.67}$$

Solving this system yields

$$R_0 = \left(\frac{\hat{\beta}}{\hat{\gamma}^3}\right)^{1/5}; \; y_0 = \left(\frac{\hat{\beta}^2}{\hat{\gamma}}\right)^{1/5}. \tag{3.68}$$

Now we are left with the following equation

$$\frac{1}{3}\tilde{R} + \tilde{y}'(\tilde{R}) = \tilde{y}^3(\tilde{R}) - \tilde{y}^3(\tilde{R})\tilde{y}''(\tilde{R}), \tag{3.69}$$

because

$$\hat{\tau}\frac{R_0^3}{y_0^4} = \frac{\hat{\tau}}{\hat{\beta}\hat{\gamma}} = \frac{\tau\lambda}{\beta\gamma} = \frac{1}{3}. \tag{3.70}$$

With our ansatz and separation of the equations, we have managed to transform the system of 4 partial differential equations into a single ordinary non-linear differential equation, which has to be numerically integrated. We have also managed to express this equation independently of detailed flow properties since we managed to rescale it so that it does not depend on any flow parameters. This equation, therefore, is general and should work for any flow in the neighbourhood of $\tilde{r}_+$.

3.5 Asymptotic behaviour

The most important quantity in the inner solution seems to be the disk semi-thickness. Hence, we will now inspect its asymptotic behaviour. We will want to match the asymptote of the inner solution as $\hat{r} \to \infty$ to the asymptote of the outer solution as $\tilde{r} \to \tilde{r}_+$. Thanks to our knowledge of $\tilde{H}_0$ in the outer solution, we will be able to check if our equations for the flow around the zero-torque radius provide correct asymptotic behaviour at large distances. We know that for the disk semi-thickness in the outer disk we can write

$$\tilde{H}_0 \sim \tilde{r}^{11/12} \left(\tilde{r}^{1/2} - \tilde{r}_+^{1/2} \right)^{1/6}, \tag{3.71}$$

which in the limit $\tilde{r} \to \tilde{r}_+$ behaves as $\hat{r}^{1/6}$, since the first term is a constant in the limit and the term in the parentheses is a linear function of $\hat{r} = \tilde{r} - \tilde{r}_+$ in the neighbourhood of $\tilde{r}_+$. Let us now examine equation (3.69) in the limit $\tilde{R} \to \infty$. We will assume that we can write $\tilde{y} \sim \tilde{R}^{\delta}$ in this limit and attempt to find the exponent δ. The equation becomes

$$-\frac{1}{3}\tilde{R} + \delta \tilde{R}^{\delta-1} = \tilde{R}^{3\delta} + \delta(\delta-1)\tilde{R}^{3\delta}\tilde{R}^{\delta-2}. \tag{3.72}$$

We can now attempt to find δ such that we compare the significance of any two terms. There are six possibilities, from which only two lead to a reasonable balancing of terms. The two possibilities are $\delta = 1/3$ and $\delta = 2$. The former leads to $\tilde{y} \sim \hat{r}^{1/3}$, which gives $\hat{H} \sim \hat{r}^{1/6}$ since our scaling of the equation does not change the asymptotic behaviour. This is the solution we are looking for, as it gives the correct behaviour of $\hat{H}$. The other possibility leads to $\hat{H}$ being linear in the limit; hence we will ignore it for now. The first possibility seems to make perfect sense as it makes the first and third term of the equation to be dominant, which is exactly what happens in the outer solution. Now with the assumption that $\hat{H} \sim \hat{r}^{1/6}$ in the limit as $\hat{r} \to \infty$, we can inspect the behaviour of the rest of the inner quantities. Starting with W, we get

$$W \sim \frac{\mathrm{d}\hat{H}^2}{\mathrm{d}\hat{r}} \sim \frac{\mathrm{d}\hat{r}^{1/3}}{\mathrm{d}\hat{r}} \sim \hat{r}^{-2/3}. \tag{3.73}$$

We now inspect how $\tilde{\Omega}_2$ behaves in the outer layer limit. The dominant term is the one with the derivative, so we only need to look at that term. We write

$$\tilde{\Omega}_2 \sim \tilde{H}_0^2 \frac{\mathrm{d}\ln \tilde{H}_0}{\mathrm{d}\ln \tilde{r}} \sim \tilde{H}_0 \frac{\mathrm{d}\tilde{H}_0}{\mathrm{d}\tilde{r}} \sim \hat{r}^{-2/3}, \tag{3.74}$$

which is in agreement with the inner quantity.

Moving on to the radial velocity. For the coefficient of the quadratic term in the vertical velocity B, we can write

$$B \sim \frac{\mathrm{d}^3 \hat{H}^2}{\mathrm{d}\hat{r}^3} \sim \hat{r}^{-8/3}, \tag{3.75}$$

where we used the fact that the denominator goes to a constant. We see that the vertical structure goes to zero rather quickly in the limit, which makes sense, as in the outer region the vertical structure plays no role in the outer limit. The dominant term independent of $\hat{z}$ is the one with the derivative, for which we write

$$\hat{H}^2 \frac{\mathrm{d} \ln \hat{H}^2}{\mathrm{d}\hat{r}} \sim \frac{\mathrm{d}\hat{H}^2}{\mathrm{d}\hat{r}} \sim \hat{r}^{-2/3}, \tag{3.76}$$

hence $\hat{v}_r \sim \hat{r}^{-2/3}$. In the outer solution we can write for the dominant term of $\tilde{v}_{r1}$

$$\tilde{v}_{r1} \sim -\tilde{H}_0^2 \frac{\mathrm{d} \ln \tilde{H}_0}{\mathrm{d} \ln \tilde{r}} \sim -\hat{r}^{-2/3}. \tag{3.77}$$

This is the only quantity that cannot be fully matched to the outer solution due to the different sign. For E we can immediately write that it is $E \sim -A/\hat{r} \sim -\hat{r}^{-5/3}$ thanks to the relation (3.52). And for F we can use equation (3.50), which gives $F \sim \hat{r}^{-11/3}$. Behaviour of the dominant term of $\tilde{v}_{z2}$ in the outer layer can be written as

$$\tilde{v}_{z2} \sim -\tilde{H}_0^2 \left(\frac{\mathrm{d} \ln \tilde{H}_0}{\mathrm{d} \ln \tilde{r}} \right)^2 \sim -\left(\frac{\mathrm{d}\tilde{H}_0}{\mathrm{d}\tilde{r}} \right)^2 \sim -\hat{r}^{-5/3}, \tag{3.78}$$

which is again in agreement with the inner solution. We see that almost all the quantities behave in the way we would expect, if we choose the solution that behaves asymptotically as $\tilde{R}^{1/3}$ for $\tilde{R} \to \infty$. The only problem is the sign in front of the dominant term of the radial velocity. It is interesting that even if we artificially add the minus in front of this term to compensate for a possible but unlikely error in calculations, the vertical velocity would then not be able to be matched to the outer one. We leave the full solution of this problem for the future work.

3.6 Analysis of the disk semi-thickness equation

As stated before, it is crucial to solve the equation (3.69) in order to obtain the structure of the disk in the boundary layer. In Section 3.5 we somewhat skipped the discussion of the two asymptotes and how we got them. Let us discuss this matter now as well as provide a numerical solution to the said equation. We begin by assuming that we can write the solution as $\tilde{y} = \kappa \tilde{R}^{\delta}$, where κ is a constant. We plug this into the equation (3.69) yielding

$$\frac{1}{3}\tilde{R} + \kappa\delta\tilde{R}^{\delta-1} = \kappa^3 \tilde{R}^{3\delta} - \delta(\delta-1)\kappa^4 \tilde{R}^{4\delta-2}. \tag{3.79}$$

We may now attempt to make any pair of the terms balanced, and we will find that the only two possibilities are $\delta = 1/3$ and $\delta = 2$. In other cases, the terms

that we are not trying to balance become dominant and we do not get dominant balance, thus we ignore these cases. The case of $\delta = 2$ gives

$$\frac{1}{3}\tilde{R} + 2\kappa\tilde{R} = \kappa^3\tilde{R}^6 - 2\kappa^4\tilde{R}^6. \tag{3.80}$$

We see that in the limit of $\tilde{R} \to \infty$, the right-hand side of this equation dominates and is balanced. We can therefore write

$$0 = \kappa^3\tilde{R}^6 - 2\kappa^4\tilde{R}^6 \Rightarrow \kappa = \frac{1}{2}. \tag{3.81}$$

Analogically we can write for the case of $\delta = 1/3$

$$\frac{1}{3}\tilde{R} + \kappa\delta\tilde{R}^{-2/3} = \kappa^3\tilde{R} + \frac{2}{9}\kappa^4\tilde{R}^{-2/3}. \tag{3.82}$$

In this case the first term on each side dominates and thus we write

$$\frac{1}{3}\tilde{R} = \kappa^3\tilde{R} \Rightarrow \kappa = \left(\frac{1}{3}\right)^{1/3}. \tag{3.83}$$

3.7 Numerical solution

In the previous section we have found two possible asymptotes of the solution, but we prefer the one that behaves as $\tilde{R}^{1/3}$ as it can be likely matched to the outer disk solution. We now know how the solution should behave at large positive $\hat{R}$. We can use this knowledge to integrate this equation numerically. To do this, we have implemented the problem in Python and used numerical routines from SciPy package. In order to analyse the general properties of the equation, we have explored the solution with the other asymptotic behaviour as well. As we deal with a second-order equation, we will need two conditions for each of the solutions. For the case of $\delta = 1/3$ we use $\tilde{y} = (\tilde{R}/3)^{1/3}$ and its derivative is $\tilde{y}' = \tilde{R}^{-2/3}/3^{4/3}$. Similarly for $\delta = 2$ we can write $\tilde{y} = \tilde{R}^2/2$ and its derivative $\tilde{y}' = \tilde{R}$. We now have to choose $\tilde{R}$ sufficiently large and let the program calculate. See Figure 3.2 for the numerical solution given by boundary conditions of the asymptote $\tilde{R}^2/2$ and Figure 3.3 and 3.4 for the other solution.

We have used the backward differentiation formula and the Adams method built-in to scipy.integrate to solve the equation numerically. Both these methods yielded the same results. We can consider our error sufficiently small to show that the solution behaves asymptotically as $\tilde{R}^2/2$. In the Figure 3.2 we have integrated from "inside", but if we were to integrate from "outside", i.e. if we set the boundary condition at, say, $\tilde{R} = 150$ and integrated inwards, we would find that the numerical solution diverges in the neighbourhood of $\tilde{R} = 1$. This behaviour is not that unexpected as we know that the solution should be valid for $\tilde{R} \to \infty$. A more interesting behaviour is the one of the numerical solution given by $(\tilde{R}/3)^{1/3}$ as it seems to diverge for any boundary condition. If we were to integrate further than in the figures provided, the numerical integration would crash. This behaviour is really unexpected, and we cannot at the moment fully explain why this happens. Strangely, this happens for both integrations, outwards as well as inwards. Unsurprisingly, this solution diverges from the asymptote more

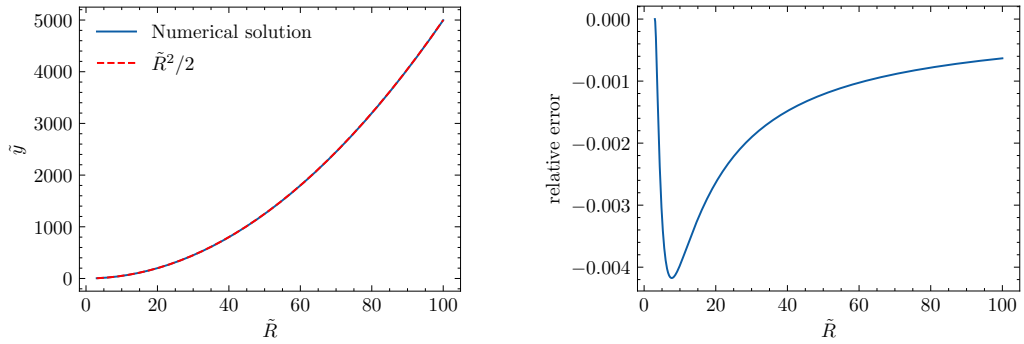

(a) Numerical solution (b) Relative error

Figure 3.2: The numerical solution of the square of the normalised disk semi-thickness equation. Left panel shows the numerical solution of the equation corresponding to the asymptote $\tilde{R}^2/2$. The equation has been integrated from $\tilde{R} = 3$ to larger $\tilde{R}$. Right panel shows the relative error of the integration as function of $\tilde{R}$. We calculated the error as $\tilde{y}(\tilde{R})/(\tilde{R}^2/2) - 1$, where $\tilde{y}\left(\tilde{R}\right)$ is the numerical solution.

slowly as $\tilde{R} \to \infty$, so it is reasonable to assume that in the limit, this solution is asymptotically correct. It is interesting to see that the other solution behaves so well, even when using the boundary condition at such a small $\tilde{R}$. If we were to choose $\tilde{R} > 3$ and integrate outwards, the relative error would shrink.

We have attempted to get rid of the divergence in the numerical calculations by introducing a new parametrisation in the following form:

$$\tilde{R} = \tilde{R}(t);\ \tilde{y} = \tilde{y}(\tilde{R}(t)), \tag{3.84}$$

which essentially made the system of two ODEs we were integrating into a system of 3 ODEs. However, this did not bear any better results.

Let us now take a step back and look back at Figure 3.1. It is possible that $\tilde{R}$ is negative, but our results may not match the inner boundary condition given by the azimuthal frequency of the star Ω_*, which would mean that there are nested boundary layers (see Bender and Orszag [1999]). If we make the same analysis we did when deriving asymptotes of the equation (3.69), we find that the only feasible solution is the quadratic one, as the other one is negative. Negative $\tilde{y}$ clearly does not make sense as it would imply that the square of the disk semi-thickness is negative. We can now try to integrate the equation numerically for negative values of $\tilde{R}$, see Figure 3.5. We can see that if we integrate from the negative values of $\tilde{R}$, we can actually integrate to the positive values; however, it is not possible to do this the other way around, which is rather strange. The difference between the numerical solution and the asymptote behaves in a completely opposite way than for the integration in the positive values – the further away we get from the boundary condition, the more significant the difference becomes. The difference is negligible for the integration towards $-\infty$, and if we integrate into the positive values, we do not really mind the error, because we prefer the other asymptotic solution due to boundary conditions given by the outer disk solution. The negative solution seems reasonable as it is not zero at $\tilde{R} = 0$, see Figure 3.5b, which corresponds to $\tilde{r}_+$, where the disk semi-thickness

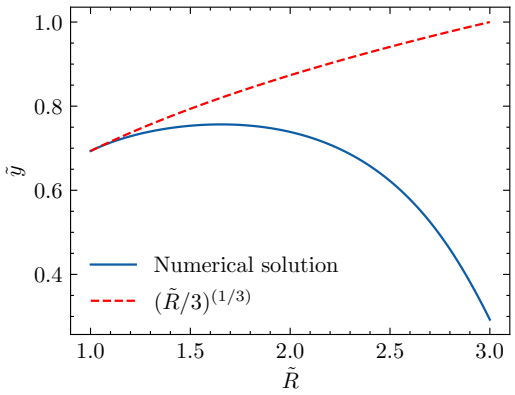

(a) Boundary condition at $\tilde{R} = 1$

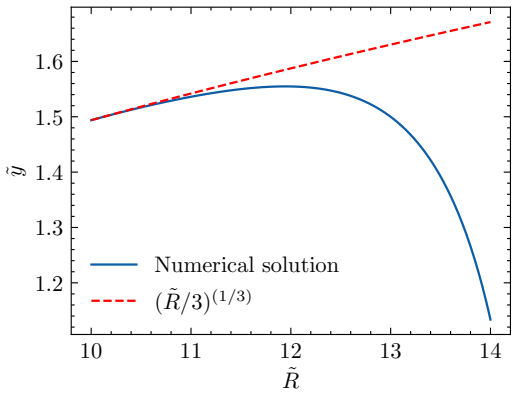

(b) Boundary condition at $\tilde{R} = 10$

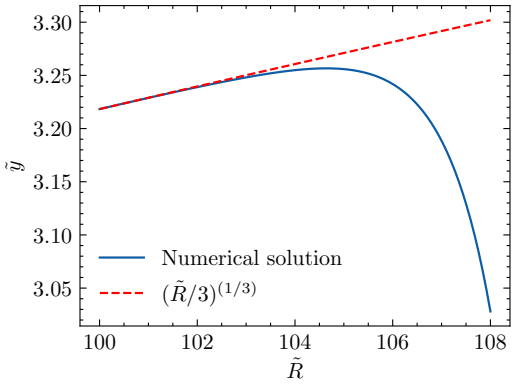

(c) Boundary condition at $\tilde{R} = 100$

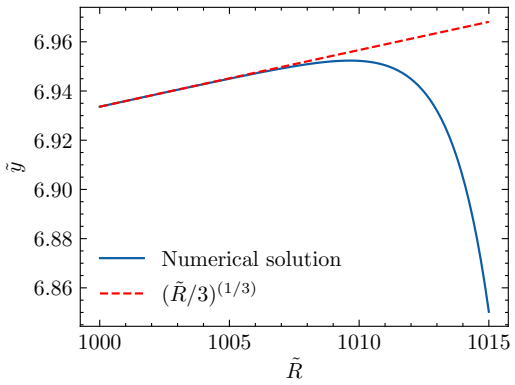

(d) Boundary condition at $\tilde{R} = 1000$

Figure 3.3: Numerical integration outwards with the boundary condition given by the asymptote of $(\tilde{R}/3)^{1/3}$.

went to zero from the outer solution. Let us now look at what the quantities look like with the assumption that $\tilde{R}^2/2$ is a good enough approximation for negative values of $\tilde{R}$. First, we need to transform our variables back to y and $\hat{r}$. We can write

$$\tilde{y} = \frac{y}{y_0} = \frac{\tilde{R}^2}{2} \Rightarrow y = \frac{y_0 \hat{r}^2}{2R_0^2} = 3\hat{r}^2, \tag{3.85}$$

where we used the relation (3.68) to plug in for R_0 and y_0. We thus know that

$$\hat{H}^2 = 3\hat{r}^2. \tag{3.86}$$

We can now calculate for W from the equation (3.46) as

$$\hat{\omega} = W = \frac{3\tilde{\Omega}_0 \hat{r}}{2\tilde{r}_+}, \tag{3.87}$$

which is negative for $\hat{r} < 0$. This makes perfect sense, because if we look at the definition of $\hat{\omega} = \hat{\Omega} - \tilde{\Omega}_K$ and realise that the stellar azimuthal frequency Ω_* is smaller than the Keplerian frequency $\Omega_K(R_*)$ at the stellar radius R_*. We can calculate the vertical velocity from equation (3.49) as

$$\hat{v}_r = 2\hat{\alpha}\tilde{\Omega}_0 \hat{r}, \tag{3.88}$$

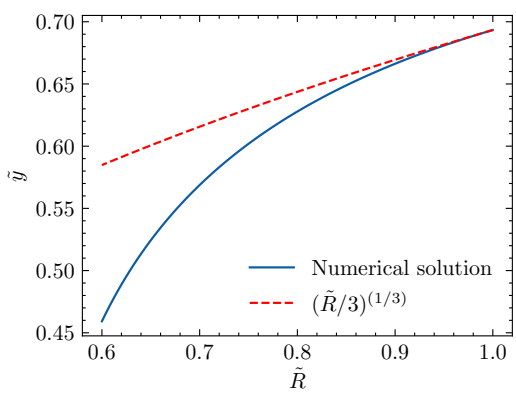

(a) Boundary condition at $\tilde{R} = 1$

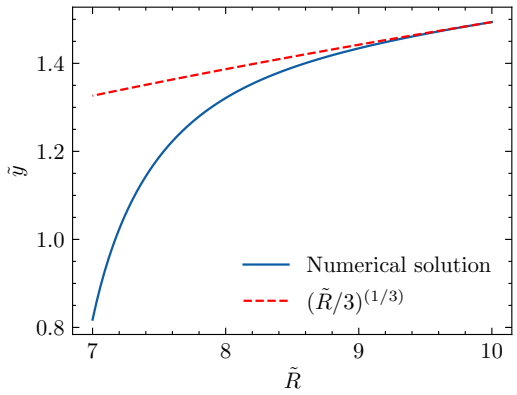

(b) Boundary condition at $\tilde{R} = 10$

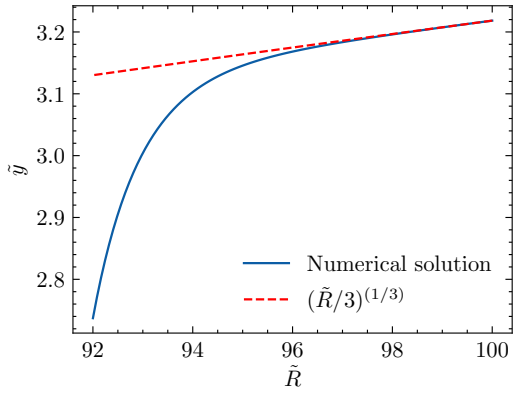

(c) Boundary condition at $\tilde{R} = 100$

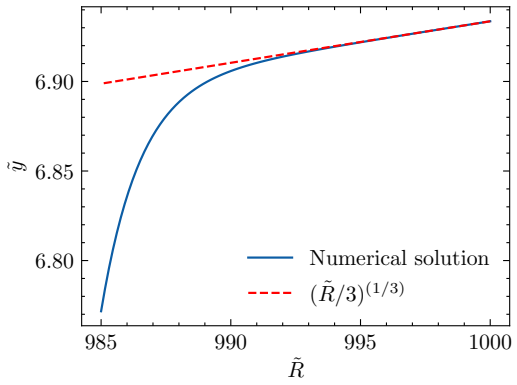

(d) Boundary condition at $\tilde{R} = 1000$

Figure 3.4: Numerical integration inwards with the boundary condition given by the asymptote of $(\tilde{R}/3)^{1/3}$.

which is also negative for $\hat{r} < 0$, implies no back-flows, and it does not depend on $\hat{z}$. Finally, we calculate from equations (3.51) and (3.52) for vertical velocity, which is a constant in $\hat{r}$ given by

$$\hat{v}_z = -8\hat{\alpha}\hat{\Omega}_0\hat{z}. \tag{3.89}$$

The solution for $\hat{\omega}$ is exciting since if we know what Ω_* is and the stellar radius is close to $\tilde{r}_+$, such that we do not have to do the limit $\hat{r} \to -\infty$, but instead say that the stellar radius corresponds to a certain $\hat{r}_*$ we can get a relation between $\tilde{r}_+$ and the azimuthal frequency of the star, i.e. the zero-torque radius will be given by Ω_*. If this is not the case, we would probably have to investigate yet another boundary layer, with given outside boundary conditions by our solution and with the inner boundary condition given by Ω_*. This may all seem very exciting, but one has to keep in mind that this prescription for the disk semi-thickness is not an analytic solution. This can be shown by plugging it into the continuity equation in $\hat{z}^2$, which cannot be satisfied with this $\hat{H}$. This can be further investigated in future works, as well as the problem of possible nested boundary layers. If we calculate for the second boundary layer, we will need to match the solutions again, and it is then when this solution comes in handy since we will want to match the innermost solution to the one, we mentioned just now. One might also attempt to come up with a smarter way of integrating the semi-thickness

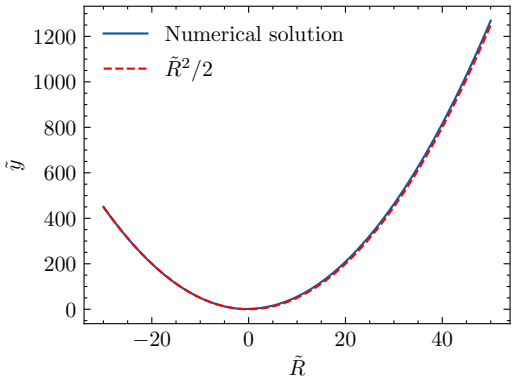

(a) Boundary condition at $\tilde{R} = -30$, integration towards the positive values

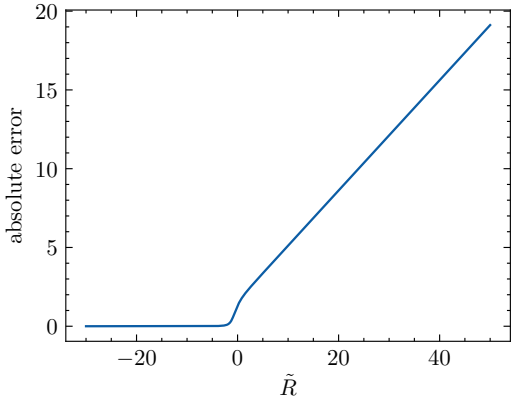

(b) The difference of the numerical solution and the asymptote

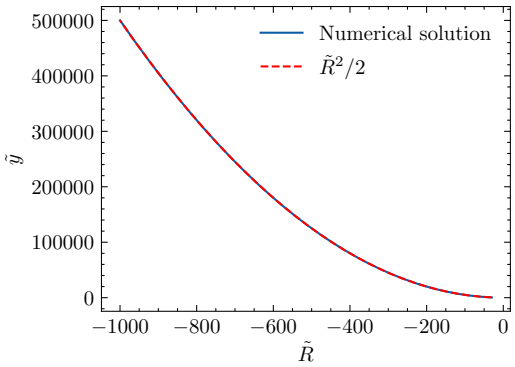

(c) Boundary condition at $\tilde{R} = -30$, integration towards $-\infty$

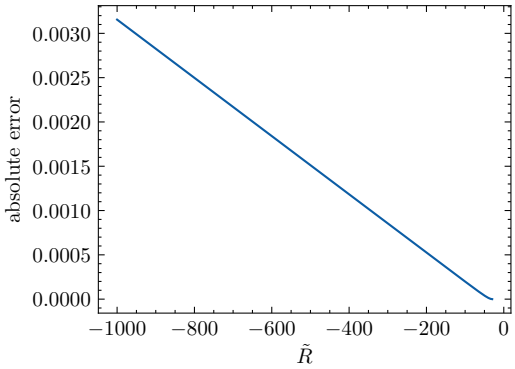

(d) The difference of the numerical solution and the asymptote

Figure 3.5: Numerical integration for negative values of $\tilde{R}$ with the boundary condition given by the asymptote of $\tilde{R}^2/2$.

equation (3.69), as the divergence might be caused by accumulating numerical errors. It could also just be the nature of this equation.

Conclusion

In this thesis, we have reviewed known results for an α–disk (Chapter 1 and 2). These results are valid sufficiently far away from the inner edge of the disk. This solution led to a singularity at the zero-torque radius $\tilde{r}_+$. In order to describe the boundary layer at the inner edge of the disk, we have discussed the origin of the singularity, which guided us to a rescaling of our variables (Section 3.2). The first attempt at rescaling was not successful as we only got a trivial solution. This might have been caused by our ansatz being too simple as the dependence on the vertical coordinate might be more complicated than we assumed. Considering this, we came up with the idea to also rescale the α parameter (Section 3.3). We were motivated to do this by the fact that the α parameter has to be less than one and also this way we eliminated the problematic term in our equations. We left the scaling factor of α as a free parameter with only one constraint – the vertical and radial velocities had to be subsonic. This greatly simplified the equations, making them analytically tractable. We have tried to employ an ansatz for the inner variables, which was motivated by the outer disk behaviour of the quantities. The first ansatz led to a trivial solution, so we needed to add vertical structure for the vertical and the radial velocity (Section 3.4). We finally obtained the same number of variables as equations, making the system solvable. Afterwards, we took a shortcut, and instead of solving the full system, which would result in a non-linear fourth-order ODE, we expressed all the variables as functions of the disk semi-thickness. Additionally, we found a lower-order equation for the disk semi-thickness from the constants of integration.

The equation for the disk semi-thickness is a single non-linear ordinary differential equation of second order. Next, we have managed to rescale the equation in such a way, that it is independent of any parameters describing the flow, therefore it is a general equation for any flow. Since we have managed to express all the variables as functions of the disk semi-thickness, solving this equation is sufficient to obtain the complete structure in the boundary layer around $\tilde{r}_+$.

Unfortunately, we were not able to find an analytical solution. Nevertheless, we were able to explore the asymptotes of this equation and find that one of the two possible asymptotes leads to an asymptotic behaviour corresponding to the outer solution, apart from the strangely behaving radial velocity (Section 3.5 and 3.6). Hence this solution can almost entirely be matched to the outer solution.

We then provided numerical solutions, which showed that the numerical solution given by our preferred asymptote diverges for any choice of boundary conditions we had tried (Section 3.7). The other solution, on the other hand, is very precise as it almost perfectly matches its asymptote but cannot be integrated backwards into negative values of the radial coordinate. However, it is possible to integrate from the negative values into the positive and it is the only feasible asymptote in the negative values. Thus, we assumed that we can take the quadratic solution of the equation in the negative values, and we calculated all the quantities for values of radial coordinate smaller than $\tilde{r}_+$. In future works, it might be necessary to use a different scaling in order to study the disk behaviour very close to the star. Nevertheless, it is possible to use the results from this work in order to match these solutions since there might be nested boundary layers.

We can summarise the achievements of this work in a few final remarks:

- We have found a scaling such that we got rid of the singularity and we managed to keep the radial and the vertical velocities subsonic, which is a common requirement imposed on self-consistent models of accretion-disk boundary layers. This scaling holds even if α is almost of the order of unity, as we have shown, that it holds for any $q > 0$. So, we might be able to extend the solution for the case of $q = 0$, which would mean no scaling of α.

- Our arguments led to scaling the radial and vertical coordinates to be of the same order. This might not be very clear when looking at the rescaling itself but one has to realize that we were rescaling the outer disk quantities, where the vertical coordinate is of order higher than the radial coordinate. This corresponds to the boundary layer thickness being of the same order as the disk thickness in the boundary layer. The same result is obtained by Shakura and Sunyaev [1988]. However, the literature seems to disagree a bit in this topic as, for example, Bisnovatyi-Kogan [1994] assumes that the boundary layer thickness is much smaller than the typical disk thickness. The scaling also gave us a relation between the orders of the velocities in the boundary layer. It says that the vertical velocity is of the same order as the radial velocity in the boundary layer which is not true in the outer disk.

- We managed to reduce the complicated system of 4 partial differential equations into a single non-linear ordinary differential equation. We have then been able to rescale this equation, such that it is independent of any flow parameters making it a universal equation for any flow in the boundary layer of a standard α-disk.

- We have been able to inspect the asymptotes of this equation and found that one matches the outer solution, except a sign in front of the radial velocity. This gave us some hints that our scaling makes sense and is correct but there also might be something we have missed as the sign in front of the radial velocity is crucial for accretion. This way our solution suggests only backflows in the boundary layer. We were able to show this only using asymptotic analysis of the equation, as we could not find the solution to our ODE due to its non-linearity. The rather strange behaviour of the numerical solutions is a subject for another works. The other asymptotic solution is not able to fulfil the equations, however, it matches the numerical solution with excellent precision. The physical nature of this asymptote is also a subject for future works as well as inspection of the possibility of nested boundary layers. The nested boundary layer might be the cause of this asymptote's inability to solve the equations since if there is the secondary boundary layer, the solution does not get far enough for the asymptote to take place. This would mean, that there is another point $\hat{r}_{++}$ in whose neighbourhood arises the nested boundary layer. This radius may be the stellar radius. Regev and Bertout [1995] also discuss the nested boundary layer, so it might be worthwhile investigating this possibility.

Bibliography

M. A. Abramowicz, B. Czerny, J. P. Lasota, and E. Szuszkiewicz. Slim Accretion Disks. *apj*, 332:646, September 1988. doi: 10.1086/166683.

W. Baade and F. Zwicky. On Super-novae. *Proceedings of the National Academy of Science*, 20(5):254–259, May 1934. doi: 10.1073/pnas.20.5.254.

C.M. Bender and S.A. Orszag. *Advanced Mathematical Methods for Scientists and Engineers I: Asymptotic Methods and Perturbation Theory*. Advanced Mathematical Methods for Scientists and Engineers. Springer, 1999. ISBN 9780387989310.

G. S. Bisnovatyi-Kogan. Analytical Self-Consistent Solution for the Structure of Polytropic Accretion Discs with Boundary Layers. *MNRAS*, 269:557, August 1994. doi: 10.1093/mnras/269.3.557.

J. Frank, A. King, and D. Raine. *Accretion Power in Astrophysics*. Cambridge University Press, 3rd edition, 2002. doi: 10.1017/CBO9781139164245.

R. Hōshi. Basic Properties of a Stationary Accretion Disk Surrounding a Black Hole. *Progress of Theoretical Physics*, 58:1191–1204, 1977.

S. Kato, J. Fukue, and S. Mineshige. *Black-Hole Accretion Disks — Towards a New Paradigm —*. Kyoto University Press, 2008.

W. Kluźniak and D. Kita. Three-dimensional structure of an alpha accretion disk. *arXiv*, 2000. doi: 10.48550/arxiv.astro-ph/0006266.

L. D. Landau and E. M. Lifshitz. *Fluid mechanics*. Pergamon Press, 1959.

Ramesh Narayan and Insu Yi. Advection-dominated Accretion: A Self-similar Solution. *apjl*, 428:L13, June 1994. doi: 10.1086/187381.

Salvatore Orlando. Low-mass x-ray binary (lmxb), Feb 2020. URL `https://sketchfab.com/3d-models/low-mass-x-ray-binary-lmxb-5bcff94396d34cca9209f2177a110d42`.

L. Prandtl. 7. Bericht über Untersuchungen zur ausgebildeten Turbulenz. *Zeitschrift Angewandte Mathematik und Mechanik*, 5(2):136–139, January 1925. doi: 10.1002/zamm.19250050212.

O. Regev. The disk-star boundary layer and its effect on the accretion disk structure. *A&A*, 126:146–151, 1983.

O. Regev and C. Bertout. Asymptotic models of accretion disc boundary layers. *Monthly Notices of the Royal Astronomical Society*, 272(1):71–79, 01 1995. ISSN 0035-8711. doi: 10.1093/mnras/272.1.71. URL `https://doi.org/10.1093/mnras/272.1.71`.

N. I. Shakura and R. A. Sunyaev. Black holes in binary systems. observational appearance. *A&A*, 24:337–355, 1973.

N.I. Shakura and R.A. Sunyaev. The theory of an accretion disk/ neutron star boundary layer. *Advances in Space Research*, 8(2):135–140, 1988. ISSN 0273-1177. doi: https://doi.org/10.1016/0273-1177(88)90396-1.

O.M. Umurhan, A. Nemirovsky, O. Regev, and G. Shaviv. Global axisymmetric dynamics of thin viscous accretion disks. *A&A*, 446(1):1–18, 2006.